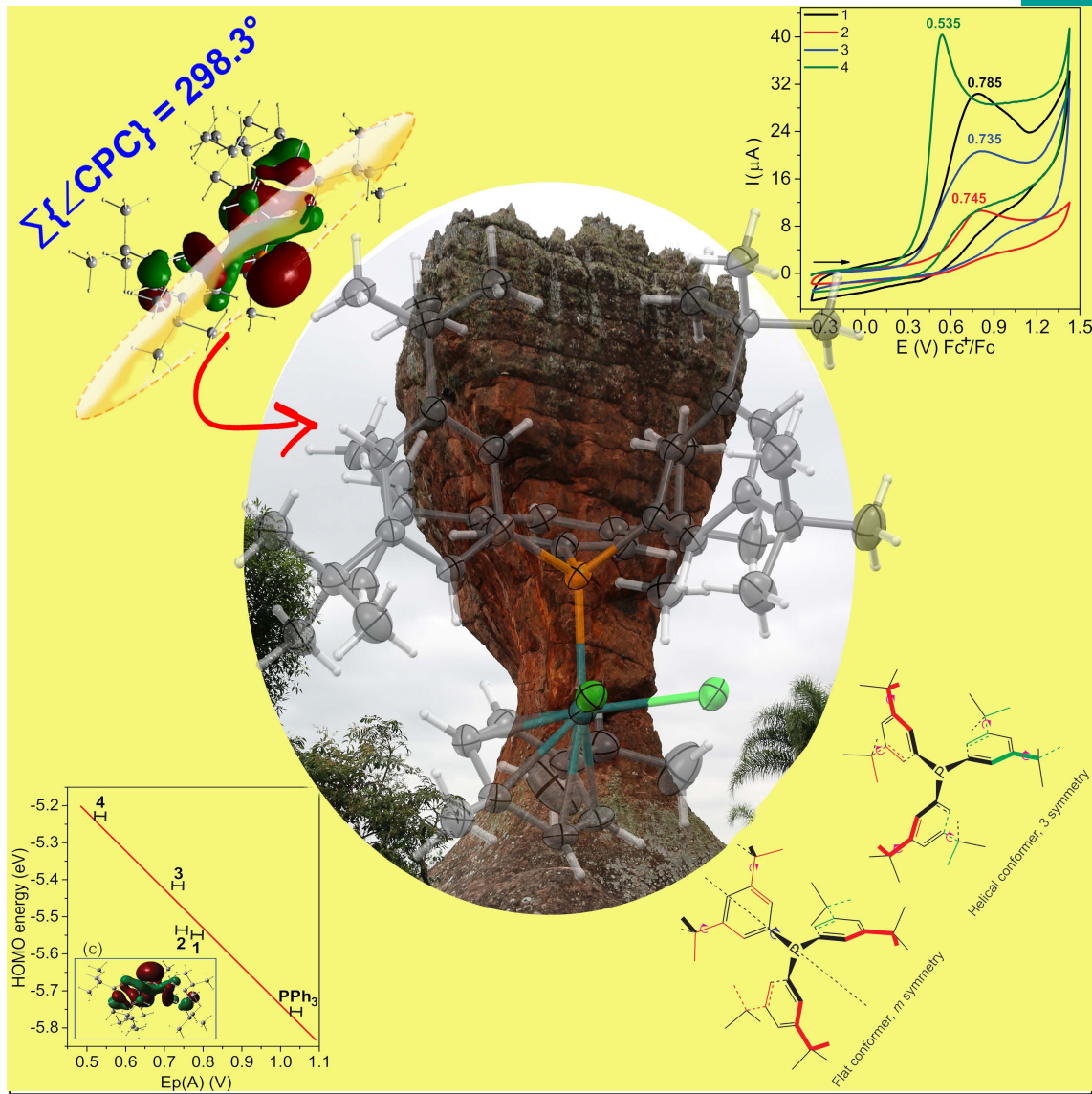




EurJIC

European Journal of
Inorganic Chemistry

A Journal of



Front Cover

###

###

WILEY-VCH

DOI: 10.1002/ejic.201501448

Read the full text of the article at 10.1002/ejic.xxxxxxx

Chemical and Electrochemical Oxidation of *Tris(3,5-di-tertbutylphenyl)phosphine* – High Z' Crystal Structures and Conformational Effects Associated with Bulky *meta* Substituents


 Ivelise Dimbarre
 Lao Guimarães

 Flávia
 Marszałkowski

 Jarem Raul
 Garcia


Karen Wohnrath



René Boeré


 University of
 Lethbridge


Invited for the cover of this issue is the group of Karen Wohnrath of the Universidade Estadual de Ponta Grossa (Paraná, Brazil) and collaborator René Boeré of the University of Lethbridge (Alberta, Canada) focused on enhancing ruthenium metallodrug design for antiproliferative and antibacterial agents. Highly lipophilic organophosphines, such as the title compound, show great promise for these applications.

In one word, how would you describe your research?

Inspiring! Group members are chiefly chemists but work with an interdisciplinary team assembled by Karen Wohnrath – synthetic chemists, electrochemists, crystallographers, computational chemists, and cell biologists, drawn from several Brazilian Universities and from Canada – to push the boundaries of current metallodrug design, focusing on arene-ruthenium complexes containing fixed and solvent-replaceable ligands.

How did the collaboration on this project start?

The principal investigators got to know each other when both were visiting a mutual colleague's lab on research leaves. We thought there would be an opportunity to share our strengths and sought collaborative funding from the Science Without Borders initiative of the Brazilian Science Foundation (CNPq) – successfully!

What is the most significant result of this study?

While searching for lipophilic phosphines as supporting ligands for neutral and cationic (η^6 -arene) ruthenium(II)L_xPAR₃ complexes, we identified the title compound as providing an intriguing balance between distal steric effects and highly lipophilic character from the heavy *t*butyl group substitution. What we did *not* expect was the attending strong intramolecular dispersion forces with effects on structure and donor strength. This leads to an unusual increased pyramidality. But we can also anticipate strong lipophilic attraction to cell membranes of complexes containing such phosphines through *intermolecular* dispersion forces.

Does the research open other avenues that you would like to investigate?

Whereas the original focus was on cytotoxicity, an application for which arene-ruthenium organometallic complexes have long been investigated, we have also discovered promising antibacterial action by neutral phosphine-supported derivatives. The mechanisms of the diverse biological activity of these complexes are under investigation using a variety of biological and physical tests. Membrane interactions are also being studied using Langmuir films, a special expertise of the team. As electrochemists, we have paid attention to the redox stability of our target complexes under physiological conditions.

What are the main challenges in the broad area of your research?

The challenges to develop new inorganic metallodrugs are immense – it takes a very active imagination to consider the effects of the *in vivo* conditions on organometallic complexes. Solubility is a major consideration as intra- and extracellular fluids are so different from those employed in synthesis and traditional characterization methods. Even detecting the metal in the cancer or bacterial cells is a major challenge as therapeutic levels translate into very low concentrations. The use of a team approach is therefore essential to provide the needed expertise.

Who pays the bill for the research highlighted on the cover?

Funding was provided by CNPq and CAPES (Brazil) and NSERC-Canada.



What was the inspiration for this cover design?

“The goblet” – one of many striking red sandstone formations in Vila Velha ('old village') State Park near Ponta Grossa – is a favourite local attraction. It seems to model the *distal steric bulk* of our phosphines, especially when they are coordinated as supported ligands in representative metal complexes.



Chemical and electrochemical oxidations of *tris(3,5-di-*tert*-butylphenyl)phosphine*. High Z' crystal structures and conformational effects associated with bulky *meta* substituents.

Ivelise Dimbarre Lao Guimarães,¹ Jarem Raul Garcia,¹ Karen Wohnrath*¹ and René T. Boeré*^{2,3}

¹ Departamento de Química, Universidade Estadual de Ponta Grossa 84030-900, Ponta Grossa, Paraná, Brazil

² Department of Chemistry and Biochemistry, University of Lethbridge, Lethbridge, Alberta T1K 3M4, Canada

³ Canadian Centre for Advanced Fluorine Technologies, University of Lethbridge, Lethbridge, Alberta T1K 3M4

Abstract

Synthesis and single crystal X-ray diffraction structures of $(3,5\text{-}^t\text{Bu}_2\text{-C}_6\text{H}_3)_3\text{P}$, $(3,5\text{-}^t\text{Bu}_2\text{-C}_6\text{H}_3)_3\text{PO}\cdot\text{H}_2\text{O}$, $(3,5\text{-}^t\text{Bu}_2\text{-C}_6\text{H}_3)_3\text{PS}$ and $(3,5\text{-}^t\text{Bu}_2\text{-C}_6\text{H}_3)_3\text{PSe}$ are reported. The structure of $(3,5\text{-}^t\text{Bu}_2\text{-C}_6\text{H}_3)_3\text{P}$ has $Z' = 4$, with both *M* and *P* enantiomers of a helical conformation and a conformation with one flat ring in the same lattice. The pyramidality index, $\sum\{\angle\text{CPC}\}$, is smaller for the helical compared to the flat conformers. All four have structures that are more pyramidal than the corresponding $\text{Ph}_3\text{P(E)}$ derivatives, which is attributed to stronger intramolecular dispersion forces. The oxide crystallizes with $Z' = 2$ as a water-bridged dimer that is the most separated such dimer amongst 26 known structures, providing evidence for a distal (or perimeter) steric effect. Cyclic voltammetry in $\text{CH}_3\text{CN}/[^t\text{Bu}_4\text{N}][\text{ClO}_4]$ indicated anodic peak potentials of +0.785 V for $(3,5\text{-}^t\text{Bu}_2\text{-C}_6\text{H}_3)_3\text{P}$, +0.745 for $(3,5\text{-Me}_2\text{-C}_6\text{H}_3)_3\text{P}$, +0.735 V for $(4\text{-MeO-}3,5\text{-Me}_2\text{-C}_6\text{H}_3)_3\text{P}$ and +0.535 V for $(4\text{-MeO-C}_6\text{H}_3)_3\text{P}$, all relative to $\text{Fc}^{+/-}$. On this scale, Ph_3P oxidizes at +1.04 V. The unexpectedly high oxidation potentials for the first three phosphines is attributed to a more pyramidal structure resulting in lowering of the HOMO energy compared to expectations from Hammett constants and ${}^1\text{J}(\text{P},\text{Se})$ NMR coupling constants.

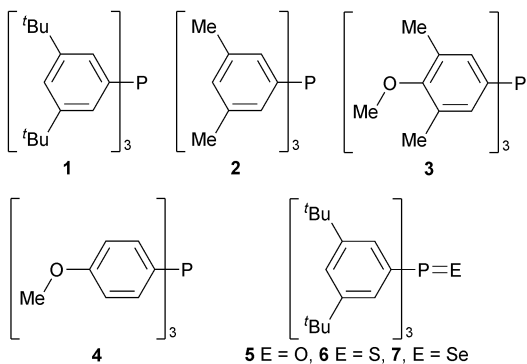
Keywords:

triarylphosphane; donor strengths from voltammetry; racemization of propeller molecules; London dispersion forces; empirical dispersion corrections

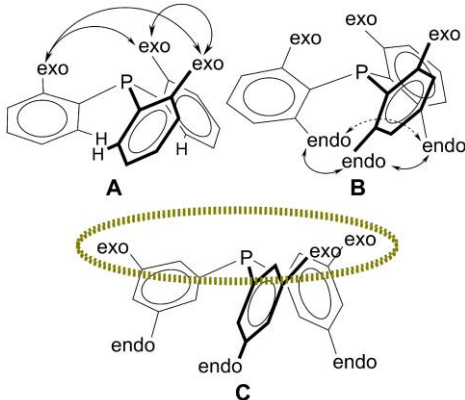
Introduction

Phosphines remain amongst the most important ligands in transition metal coordination and organometallic chemistry with applications to catalysis,¹⁻⁴ are very important Lewis bases for frustrated Lewis pair (FLP) chemistry⁵ and are used in critically important organic processes such as the Mitsonobu reaction.⁶ Triarylphosphines are still the most diverse and commonly employed phosphines. Molecules in the class Ar₃P and Ar₃P=E (E = O, S, Se) have long been important to the isomerization and energetics of propeller-shaped molecules based on foundational work of Mislow on triarylmethanes.⁷⁻⁹ His group established the strong connection of experiment (originally from dynamic NMR spectroscopy) with pioneering work in computational stereochemistry.¹⁰ Interest in this area remains strong amongst triarylphosphines,¹¹⁻¹⁴ triarylphosphine chalcogenides,^{15,16} and conformations of Ar₃P ligands in coordination complexes.¹⁷⁻²¹

We are exploring a series of substituted triarylphosphines **1** - **4** with different donor strengths and hydrophobicity.²² Whereas **2** – **4** are commercially available,²³⁻²⁵ the title phosphine *tris*(3,5-di-*tert*-butylphenyl)phosphine, **1**, was, at the time our study commenced, only reported in a single communication and remained incompletely characterized.⁴ In particular, the crystal structure has not been reported.



Our extensive experience with hydrophobic phosphines bearing bulky 2,6-substituents, such as *tris*(2,6-diisopropylphenyl)phosphine (Dipp₃P),^{26,27} *tris*(2,4,6-triisopropylphenyl)phosphine (Tripp₃P)²⁸ and *tris*(2,4,6-trimethylphenyl)phosphine (Mes₃P),²⁹ was not transferable to our target ruthenium complexes as they are too sterically congested to coordinate to the metal and we thus turned to analogous 3,5-disubstituted ligands. We were particularly attracted to **1** and **2** but for completeness included 4-MeO substituted phosphine **3** and the corresponding **4** (which is one of the most basic Ar₃P). Solution redox potentials have been recognized as excellent measures of phosphine donor ability and thus the voltammetric behaviour of the series **1** – **4** have been determined.^{26,27,30-32} Since chalcogenides of **1** were not known and no crystal structures of the series **1**, **5** – **7** has been reported, we synthesized them all and determined their structures to obtain pyramidalities indices (i.e. the sum of the angles around phosphorus, $\sum\{\angle CPC\}$)³³ for comparison to bulky 2,6-disubstituted phosphines.²⁶⁻²⁹ It is now recognized that different types of steric effects can occur in pyramidal phosphines. Systematic substitution in the 2-position provides *steric shielding* (Scheme 1A) by creating a cavity around the Lewis-basic electron density of the highest occupied molecular orbital (HOMO). This occurs when all the substituents are oriented *exo*, as is commonly but not exclusively observed in coordination complexes.³³ However, systematic 2,6-disubstitution also generates *steric pressure* (Scheme 1B) between the *endo* substituents. This repulsive interaction can significantly decrease the pyramidalities of PAr₃, which raises the HOMO energy (inducing greater basicity) and enhances the steric shield by forcing the *exo* substituents closer around the phosphorus donor.^{26,33} Systematic 3-substitution provides an opportunity for the flanking *exo* groups to create a coordination pocket (dashed perimeter in Scheme 1C) without direct interference with the donor site (distal steric bulk).³⁴⁻³⁷ But does 3,5-disubstitution also generate steric pressure from the *endo* substituents? The title compound **1** and its chalcogenides **5** – **7** can help answer this question.



Scheme 1. Steric effects in substituted PAr_3

The crystal structures of **1** and **5 – 7** proved to be challenging due to a variety of disorder phenomena, especially **1** which crystallizes from numerous solvents, as well as by sublimation, in an unusual lattice with four molecules in the asymmetric unit ($Z' = 4$). There is a growing awareness of crystal structures with values of $Z' > 1$,^{38,39} the incidence of which has steadily been rising and achieved 16% of all organic structures compiled in the Cambridge Crystallographic Database (CSD)⁴⁰ in 2016. It is likely that this increasing incidence reflects improvements in crystallographic technology (hardware and software) since structures with more than one equivalent chemical entity in the asymmetric unit are usually more difficult to solve and to refine to publication quality. Nevertheless, higher values still remain extremely rare so that the incidence of $Z' > 2$ is only 1.23% in the CSD (2016).

During the course of our work, several new papers were published which independently reported the synthesis and utilization of **1**,^{2,3,6} thus generating significant interest in a phosphine that has lain dormant for some twenty years. The main purpose of this paper is to provide evidence for the relative donor strengths for **1 – 4** and to explore steric effects from 3,5-disubstitution in the structures of **1** and its derivatives.

Results and Discussion

Synthesis. We prepared **1** by modifying the original report of Manabe to facilitate workup under anaerobic conditions, using canula techniques.⁴ Although the reactions are essentially quantitative (confirmed by NMR and mass balance), purification proved difficult and all the reported preps suffer in recovered yield.^{2,3,6} This seems to be due to the extremely high solubility of **1** in alcohols. Crystallographic investigation demonstrated that growing crystals free of oxide contamination was especially difficult (see SI for details). The oxide **5** was therefore made deliberately to confirm this contaminant spectroscopically (see below). We eventually found that recrystallization from a minimum quantity of cold 3:1 MeOH/EtOH under N_2 affords small colourless needles of pure **1**.

Crystal structure of **1.** Single crystal X-ray diffraction provides the structure of **1** which has the same habit (small colourless long thin plates) and unit cells when grown from ethanol or methanol as recrystallization solvents and also when grown by sublimation in a gradient furnace. The structure is complicated, with 4 independent molecules in the $\text{P}2_1/c$ lattice (denoted as $Z' = 4$, see Table S1 in the SI). These exist as two distinct conformational isomers; the one shown in Figure 1a has aryl ring C1 > C6 oriented 'flat', i.e. orthogonal to a plane that contains the principal axis of the whole molecule through P1 and the non-bonded electrons on phosphorus. The other three have the common helical arrangement of all three rings (Figure 1b), with approximate three-fold rotational symmetry. The two types of conformations are depicted in perspective in Figure 1c in idealized form to facilitate discussion. Additionally, within the asymmetric unit (as denoted by the phosphorus atoms), P100 has an anti-clockwise rotation (*P* configuration – see Figure S13 in the Supporting Information – SI)^{13,18,41} if viewed from above while P200,300 have clockwise rotation (*M*).⁴²

Three of the four molecules have significant rotational positional disorder of the ^tBu rings that could be modelled with part occupancies (see the SI). The independent molecules also show a distribution of limiting conformations of the ^tBu groups w.r.t. the attached aryl planes; in the four rotationally disordered groups, the components are close to these two limiting conformations. The observed (Fig. 1c) limiting conformations of the ^tBu groups have one in-plane methyl group either *syn* with the side of the phenyl ring (red colour) or *anti* (green colour).

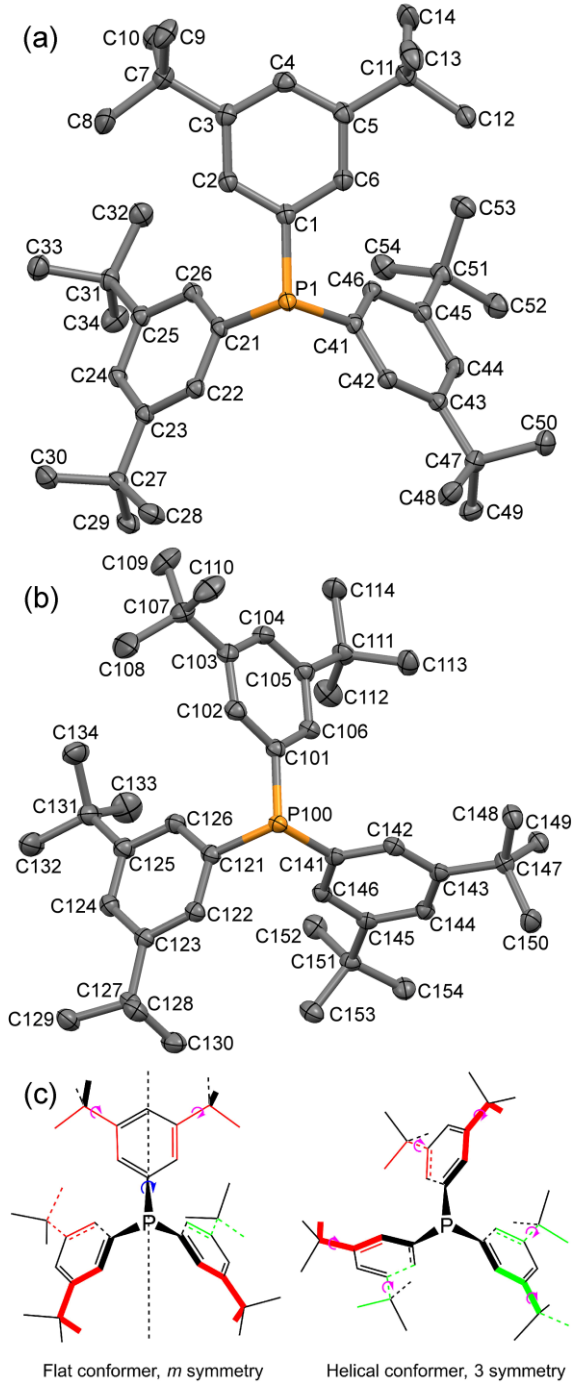


Figure 1. Displacement ellipsoids plots (30% probability) of (a) the 'flat' conformation designated by P1 containing C1→54 and (b) one of the helical conformations designated by P100. Only the major components of the two-part rotational disorder model for ^tBu groups C11 and C47 are shown. Hydrogen atoms are omitted and the atom numbering scheme of x1 – x14 for the 12 aryl rings is provided. (c) Perspective diagrams of the P1 and P300 molecules for the major ^tBu conformations in the crystal structure.

High Z' in Ar_3P and Ar_3PE . The Durham High Z' database for $Z' > 4$ ⁴³ has no entries for Ar_3P and Ar_3PE ($E = \text{O}, \text{S}, \text{Se}$). A review of the CSD entries (CSD Version 5.39, November 2017) reported 108 Ar_3P structures with $Z' = 2$ and 72 for Ar_3PO . For $Z' = 3$, there were two entries for Ar_3P and four for Ar_3PO , while for $Z' = 4$, there were just 11 Ar_3P and 5 Ar_3PO examples. Thus, the incidence of $Z' > 1$ for triarylphosphines is low both in number and range. Intriguingly, one of two polymorphs of *tris(3,5-bis(trifluoromethyl)phenyl)phosphine* (CSD refcode: IGAGIG), a close structural analogue to **1** in view of the similar molecular size of CF_3 and ^tBu substituents, also crystallizes with $Z' = 4$.^[44] Moreover, in that structure three of the four molecules are predominantly in a 'flat' conformation and only one is helical. Furthermore, unlike **5 – 7**, the oxide and selenide of this fluorinated phosphine all adopt the flat conformation in their respective crystal structures.^{45,46}

Computational analysis of conformation. It was thus important to ascertain which of the two, 'flat' or helical, is the lower energy in **1** and what the energy difference between conformers is. Hybrid DFT calculations were undertaken at the B3LYP/6-31G(2d,p) level of theory and an optimization that starts with the flat conformer as found in the crystal structure (Figure 1a) smoothly converts over to a helical geometry. The most optimized flat geometry was found to be about $6 \text{ kJ}\cdot\text{mol}^{-1}$ higher in energy than the optimized helical conformation.

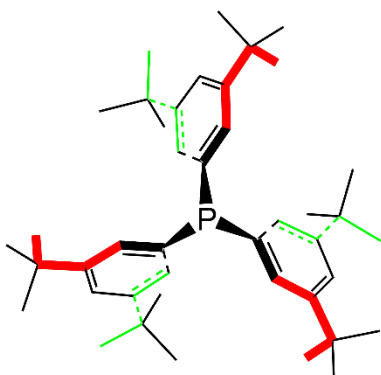


Figure 2. DFT minimum-energy conformer: symmetry point group 3, with the upper ^tBu groups oriented with a co-planar methyl group *syn* (red) and all the lower ^tBu groups oriented *anti* (green colour).

Once it was found that the helical form is the most stable, attention was paid to the limiting conformations of the ^tBu groups. Whereas in the geometry taken from the X-ray structure, five ^tBu groups are oriented with one methyl group in-plane with the attached aryl rings and in *syn* conformation and the sixth is found *anti*, the 3-fold symmetric conformation wherein all three *exo* ^tBu groups (i.e. on the phosphorus atom side of the pyramid) are *syn* and the three *endo* groups all *anti* (Figure 2) is the lowest-energy at this level of theory. By contrast, alternatives with one of the lower groups *anti* and the other two *syn* is $\sim 1.5 \text{ kJ}\cdot\text{mol}^{-1}$ higher and the more symmetric analogue with *all* the lower groups *syn* is $\sim 2.3 \text{ kJ}\cdot\text{mol}^{-1}$ higher in energy than that of the calculated lowest energy conformer. Such small energy differences are certainly consistent with the presence of rotationally disordered ^tBu groups in the reported crystal structure (see above). For the same reason it is evident that thermal energy at RT is also capable of promoting the P1 molecule found in the crystal structure of **1** to a flat conformation ($\sim 6 \text{ kJ}\cdot\text{mol}^{-1}$).

This geometry with optimal ^tBu group orientations (Fig. 2) was then used in a 'relaxed scan' algorithm by stepping one fixed C-P-C-C dihedral angle (C1-P1-C21-C26) with variable step sizes to investigate any influence of the bulky 3,5-substituents on the phosphine racemization mechanism (Figure 3). This follows the classical algorithm of Mislow for computational investigation of conformation.⁸ For comparison, a similar relaxed scan at the same level of theory was undertaken for the 'parent' phosphine PPh_3 . The scans were undertaken over approximately 180° . For PPh_3 starting from the *M* helical enantiomer, **i**, the energy rises to a maximum **ii** at about $5.6 \text{ kJ}\cdot\text{mol}^{-1}$, with a 'flat' orientation of one ring, in accordance with the determination

by Mislow that the two-ring flip is the threshold mechanism for racemization of triaryl pyramidal molecules (Figure S13).^{7,8,13} Beyond this maximum, the *P* helical structure **iii** is achieved. Further driving of the dihedrals leads to a second 'flat' conformation **iv** at 5.1 kJ·mol⁻¹, that differs slightly from **ii** in the relative twists of the other two phenyl rings and then rapidly falls off to a final helical *M* geometry **v** that is identical to **i**. None of this is surprising, but when the same scan is undertaken on the optimized geometry of **1**, starting from the *M* ground state **I**, the energy rises steeply and reaches a different maximum **II** at about 26 kJ·mol⁻¹, for which the geometry is very close to the idealized intermediate of Mislow's one-ring flip mechanism (one aryl ring parallel to the principal axis). At **III** the *P* enantiomer is attained (which can be further optimized to the same energy as **I**). Further driving of the dihedral leads to **IV** at 6.7 kJ·mol⁻¹, with the single 'flat' aryl ring. Fascinatingly, the energy barrier for the intermediates **IV** and **iv** are extremely similar despite the large differences in substituent bulk. Thus, **1** can be expected to shuttle back-and-forth over the barrier at **IV** to interconvert its chirality (and **III**, **IV** and **V** co-exist in the lattice of the $Z' = 4$ crystal structure – as discussed above).

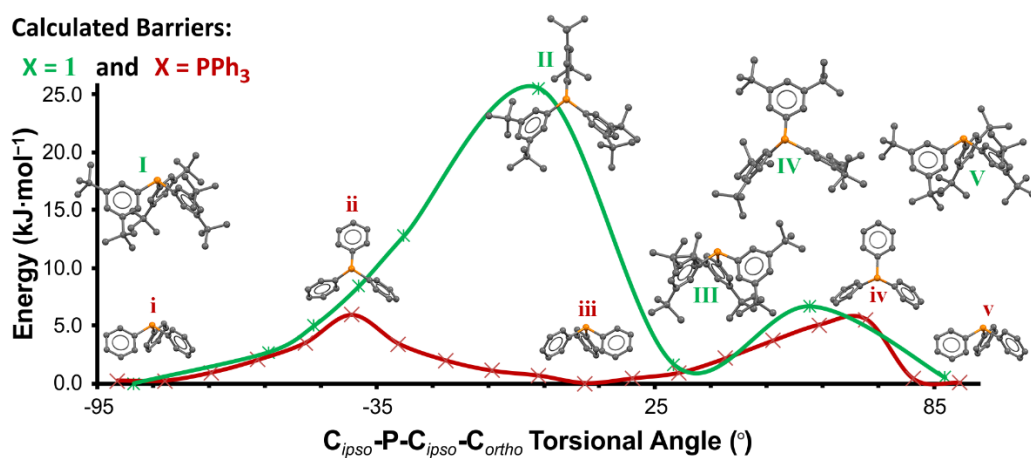


Figure 3. Comparative computed energy scans at the B3LYP/6-31G(2d,p) level of theory for **1** (green) and PPh_3 (red) with full optimization of all parameters other than the $C_{ipso}\text{-P}\text{-}C_{ipso}\text{-}C_{ortho}$ torsion angles. Molecular conformations for the energy maxima and minima are also depicted (see text for further details).

Electrochemical oxidations and phosphine donor strengths. The electrochemical properties of phosphines **1–4** and PPh_3 were studied by cyclic voltammetry (CV) in $\text{CH}_3\text{CN}/[n\text{BuN}][\text{ClO}_4]$ solutions and representative voltammograms are presented in Figure 4a. The CVs show the presence of an irreversible oxidation process with anodic peak potentials (E_p°) in the range +0.54 to +0.79 V. Scan-rate dependencies correlated linearly with the square root, indicating diffusion-controlled processes (see Figure S11). Irreversible oxidations for phosphines lacking enhanced steric shielding (Scheme 1B) is normal and has been attributed to rapid reaction with adventitious water.²⁷ Despite this, good correlations of the anodic peak potentials have been obtained to the relative basicity of phosphines.^{30–32} The range of potentials in **1–4**, 0.25 V, is reasonably large for this variation in substituents. Phosphines **2**, **4** and PPh_3 were measured previously in a comparative investigation, albeit under very different conditions (data included in Table 1).⁴⁷ These results agree well in the relative placement of **2** between **4** and PPh_3 (potential steps of 0.17 V and 0.18 V, compared to ours of 0.29 V and 0.21 V). Geometry optimized B3LYP/6-31G(2d,p) DFT calculations, incorporating Grimme's D3 empirical dispersion correction, were performed on **1–4**, and the energy of the HOMO of each phosphine is also listed in Table 1. Electrochemical oxidation involves the removal of an electron from this orbital (Figure 4c, inset). The oxidation potential data correlates linearly with the HOMO energies, yielding an R^2 of 0.97 (Figure 4b). By contrast, the Hammett σ^+ constants make the wrong prediction, especially for **3** (see Figure S12).

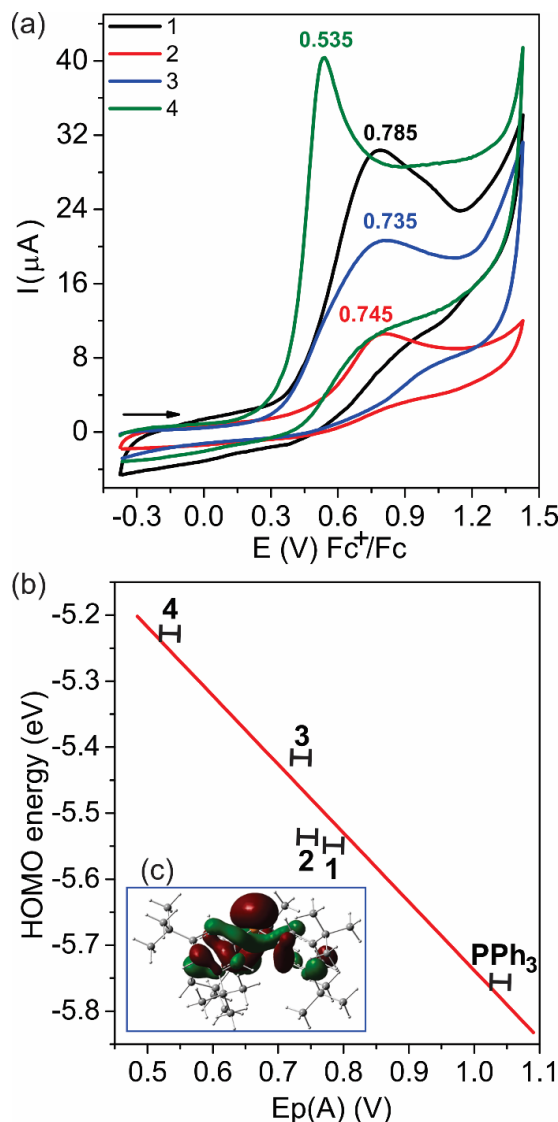


Figure 4. (a) Cyclic voltammograms of phosphines **1** - **4** in $\text{CH}_3\text{CN}/[\text{nBu}_4\text{N}]\text{[ClO}_4]$ solutions measured vs. Ag/AgCl and expressed on $\text{Fc}^{+/0}$ scale. (b) Relative basicity of **1** - **4** and Ph_3P from the correlation between E_p^a and DFT HOMO energies ($R^2 = 0.97$). (c, inset) Kohn-Sham orbital surface diagram for the redox molecular orbital of **1**.

Table 1. Experimental voltammetric data and DFT computed redox orbital energies

Phosphine	E_p^a , V ^a	ΔE to 1 , V	Culcasi, V ^b	HOMO, eV	Hammett $\sigma^+ c$	$\sum\{\angle\text{CPC}\}$, $^\circ d$
PPh_3	+1.04 ^e	-0.251	+1.40	-5.755	0	305.1
1 (<i>3,5-t</i> Bu ₂ C ₆ H ₄) ₃ P	+0.785	0.000		-5.549	-0.118	298.3
2 (3,5-Me ₂ C ₆ H ₄) ₃ P	+0.745	0.025	+1.22	-5.536	-0.132	304.8
3 (4-MeO-3,5-Me ₂ C ₆ H ₄) ₃ P	+0.735	0.039		-5.416	-0.91	304.8
4 (4-MeO-C ₆ H ₄) ₃ P	+0.535	0.251	+1.05	-5.228	-0.778	305.4

^a Measured in $\text{CH}_3\text{CN}/[\text{nBu}_4\text{N}]\text{[ClO}_4]$ solutions vs. Ag/AgCl and scaled to $\text{Fc}^{+/0}$ at the invariant internal $E_{\gamma} = +0.375$ V. Estimated error = ± 0.010 V ^b Determined by CV in *n*-butyronitrile vs. SCE.⁴⁷ ^c From ref. 48. ^d From geometry-optimized B3LYP/6-31G(2d,p) hybrid DFT calculations incorporating Grimme's D3 empirical dispersion corrections. ^e From ref. 26.

According to both the voltammetric data from our study and that of Culcasi *et al.*, as well as the calculated HOMO energies, **1** – **3** cluster together with similar donor strengths roughly half-way along the range between PPh_3 and very basic **4**. A different way to establish phosphine donor ability is the well-known correlation between one-bond ^{77}Se - ^{31}P NMR coupling constant and pK_b .⁴⁹ Since we have prepared the selenide **7** in bulk (see below), it was possible to accurately measure its coupling constant as $^1\text{J}(\text{Se}, \text{P}) = 719$ Hz. Using the empirical correlation of Beckmann *et al.* and restricting to just Ar_3P entries rather than all triorganophosphines, this provides an estimate of $pK(b) \approx 10.2$, which places **1** close to $(4\text{-CH}_3\text{C}_6\text{H}_4)_3\text{P}$ in basicity.⁴⁹ There is thus a significant discrepancy between the donor ability established from the direct Se-P coupling constant and the voltammetry.

Chemical oxidations. In addition to voltammetry, chemical oxidations of **1** were undertaken with oxygen, sulfur and selenium. Full characterization details are provided in the Experimental section and the crystal structures were determined. While this work was in progress, brief reports have appeared independently for the preparation of oxide **5**² and selenide **7**³ with partial characterization for each.

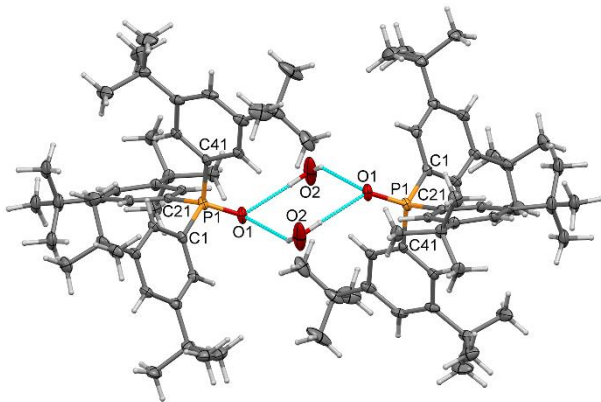


Figure 5. Displacement ellipsoids plot (40% probability) of one of the two crystallographically independent and centrosymmetric water-bridged dimers of **5** as found in the crystal lattice. H atoms not involved in H-bonding and minor components of disordered ^3Bu groups have been omitted for clarity. The water O2 atoms are centered on a plane also containing the two P1 atoms of the asymmetric unit.

The oxide crystallizes as two independent centrosymmetric water-bridged dimers ($Z' = 2$; Figure 5). However, the presence of a superlattice provides an alternative refinement with $Z' = 4$ (see Figure S3); on comparison of the two models, no significant advantage obtains from the superlattice as both models involve disorder. One of the two dimers is depicted in Figure 5 involving water atoms O2 and the P1-O1 atoms. Notably, the second dimer involving water atoms O3 and the P100-O100 atoms was found to have only 0.65 occupancy for the water and is also a less compact dimer. The O···OH₂ contact distances in the depicted dimer are 2.861(2) and 2.981(3) Å, averaging to 2.921 Å, whereas for the P100 structure the distances are 2.902(6) and 3.065(6) Å. A search of the CSD (Nov 2016) found 25 structures in which two phosphine oxide units are bridged by two water molecules in a manner analogous to **5** (see Table S3). The full range of individual contacts in this search is from 2.649 – 2.930 Å, but the average within a given structure ranges from 2.680 – 2.901 Å. By both criteria, the dimers in **5** have the longest O1···O1' distances of the set. This suggests that the steric repulsion in **5** between *meta* ^3Bu substituents on adjacent molecules of the bridged dimer is significant (for a space-filling representation of the dimers see Figure S4). In other words, this suggests the existence of distal steric effects also in **5** (see above, Scheme 1c).

The torsion angles O–P–C–C_{2,22,42} and O–P–C–C_{102,122,142} are all different: 26.7(2), 25.0(2), 35.7(7) and 31.3(2), 13.9(2), 54.3(2) so that the geometry of the P100/O100 molecule approximates to the Mislow one-ring flip intermediate (one aryl ring co-planar with the principal axis – see Figure S13).^{7,8,13} By contrast the

P1/O1 molecule is closer to helical. The average P=O distance in **5** is 1.4925(10) Å, which is identical to the average 1.494(6) Å for the 25 comparative water bridged dimers in Table S3 and perhaps slightly longer than a global average for 700 Ar₃P=O found in the CSD of 1.488(13) Å.

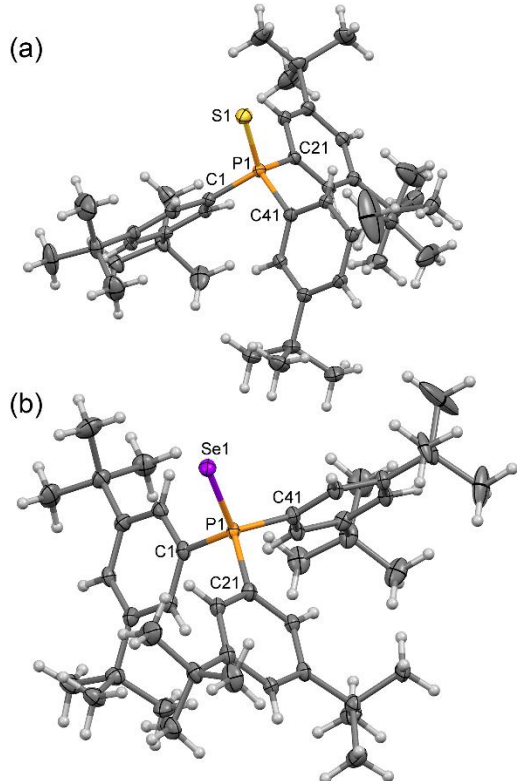


Figure 6. Displacement ellipsoids plots (40% probability) depicting the molecular structure of (a) **6** and (b) **7** as found in their crystal lattices. Minor components of disordered ^tBu groups, as well as Se and P in **7**, are omitted (see the ESI).

The crystal structures of sulfide **6** and selenide **7** are isostructural in *P*2₁/c (Figure 6). The data for **7** were determined several times but always display some strange ghosting of heavy atom sites, leading to large residual peaks in the refinement. No suitable twin law could be found to deal with this issue but the refinement as a whole-molecule disorder is otherwise unexceptional. The two structures display ^tBu disorders for the same groups, likely reflecting regions of lesser interactions in the lattice. Both lattices also contain voids (67 Å³, 1.7% of cell volume for **6**; 141 Å³, 3.5% of cell volume for **7**) but the volumes of these voids are too small to be solvent accessible. There are no significant intermolecular contacts in either structure.

The torsion angles S–P–C–C_{2,22,42} are 50.2(2), 40.7(2), 42.4(2) in **6** and Se–P–C–C_{2,22,42} are 49.7(3), 39.0(3), 44.5(3) in **7**. Thus, these essentially isostructural molecules are both closer to an ideal helical geometry with three-fold rotational symmetry than are either of the independent oxides. The P–S bond distance in **6** is 1.9596(8), which is well within the mean of 1.953(11) Å for 179 Ar₃PS reported in the CSD. The P–Se distance in **7** is 2.115(1), also entirely normal compared to the mean 2.115(14) Å for 84 Ar₃PSe in the CSD.

Phosphine pyramidality. We recently defined a pyramidality index, $\sum\{\angle CPC\}$, to help define the shapes of organophosphines and related molecules using internal geometries from crystal structures or computation.^{33,50} An index of 360° is trigonal planar and 280.8° is the almost right-angled geometry achieved in PH₃. Compared to the latter, three aryl rings cause significant reduction in pyramidality, so that for example

$\sum\{\angle CPC\} = 308.2(4)^\circ$ in Ph_3P as determined from averaging multiple crystal structures.²⁵ Advantages of this index over alternative descriptions of pyramidality include easy accommodation of deviations from full 3-fold symmetry and no need to define a principal axis.⁵² Systematic 2,6-disubstitution induces reduced pyramidality in PAr_3 , so that $\sum\{\angle CPC\} = 335.6(3)^\circ$ in Dipp_3P ,²⁶ $334.4(3)^\circ$ in Tripp_3P ,²⁸ and $329.1(5)^\circ$ in Mes_3P ,²⁹ all data taken from single-crystal diffraction studies. Pyramidality is also reduced upon oxidation, for example $\sum\{\angle CPC\}$ increases to $319.26(3)$ in Ph_3PO ,⁵³ to $317.5(4)^\circ$ in Ph_3PS ⁵⁴ and $317.9(6)^\circ$ in Ph_3PSe .⁵⁵ The pyramidality index of **1** is $303.5(2)^\circ$ for the P200,300,400 helical geometries, but $308.5(1)^\circ$ for the planar geometry of the P1 molecule in the measured crystal lattice. We can also compare $\sum\{\angle CPC\} = 313.31(5)^\circ$ in **5**, $314.69(5)^\circ$ in **6** and $315.28(10)^\circ$ in **7**. Interestingly, except for the planar geometry in **1**, *all* the *tris*(3,5-di-*tert*-butylphenyl)phosphine derivatives are consistently more pyramidal than simple $\text{Ph}_3\text{P}(\text{E})$ analogues. Thus, we can now answer the question posed in the Introduction unequivocally: *endo* 5-*t*Bu groups do not generate steric pressure. In fact, they show an attractive rather than a repulsive interaction in the *endo* region.

The most likely origins for this attraction, resulting in increased pyramidality in **1–3** and **5–7**, are dispersion forces operating between the 3,5-substituent groups and the π electron density of these electron-rich aromatic rings. In support of this notion, the DFT calculations originally used in the data analysis were repeated at the same level of theory but incorporating Grimme's D3 empirical dispersion correction with geometry re-optimization for **1–4**.^{56–60} The results have decreased values of $\sum\{\angle CPC\}$ that correlate directly with the identity of the 3,5-substituents (Table 1).²² That is, $\sum\{\angle CPC\} > 305^\circ$ for 3,5-H₂, $\sum\{\angle CPC\} = 304.8^\circ$ for 3,5-diMe (a small change) and 298.3° for 3,5-di*t*Bu (a considerably larger contraction). The role of dispersion interactions with and between 3,5-dimethylphenyl groups has recently been recognized as supplying more energy towards holding the sterically challenged all-*meta* tert-butyl hexaphenylethane together than the C–C covalent bond [59].

Conclusions

Taken together, the structural properties for **1** and **5–7** demonstrate in their crystallography the challenges posed by 3,5-*bis*-*t*Bu group substitution. Parent phosphine **1** crystallizes as a complex cluster of four molecules with several different conformations. Oxide **5** has a surprisingly strong affinity for water but has trouble maintaining the common doubly-bridged $\text{P}=\text{O}\{\text{OH}_2\}_2\text{O}=\text{P}$ motif and has the longest ever reported separation between monomers among 30 such structures, which we attribute to distal steric congestion. Moreover, the structure suffers from multiple and different types of positional disorders. The structures of **6** and **7** have voids that are not filled by solvent but indicate that the bulky shapes have difficulty filling space efficiently.

Since greater pyramidality is associated with increased *s*-orbital contribution to the HOMO, the increasing pyramidality resulting from greater London dispersion forces also provides a plausible explanation for why the basicity of **1–3** are lower than expected based on isolated-ring indicators such as Hammett σ^+ constants or from the ${}^1J_{\text{P},\text{Se}}$ coupling constants, from which changes in geometry must be excluded.⁴⁹ In view of the excellent correlation to DFT-calculated HOMO energies, we suggest that the phosphine donor strength of **1–4** established by voltammetry from anodic peak potentials are more accurate for this series than values obtained from ${}^1J_{\text{P},\text{Se}}$. The interesting possibility that the conformational profiles of **1** and PPh_3 may be significantly affected by dispersion interactions, suggested by a referee, will be further investigated and reported on at a later time.

Experimental Section

General Methods. Solvents were reagent grade or better. THF (BDH) was dried by refluxing with Na/benzophenone. *Tris*(4-methoxyphenyl)phosphine, *tris*(4-methoxy-3,5-*bis*-dimethyl-phenyl)phosphine and *tris*(3,5-*bis*-dimethyl-phenyl)phosphine (Aldrich) were used as received as was 1-bromo-3,5-*bis*-tertbutylbenzene (Aldrich). All work with air-sensitive phosphines was conducted in a dry N₂ atmosphere using modified Schlenk and vacuum line techniques. Elemental analyses for C, H, N, S were performed with a Vario Micro-cube Elemental Analyzer. FT-IR spectra were recorded on a Bruker Tensor 37 Spectrometer in the range of 4000-400 cm⁻¹. UV-Vis spectra (0.10 mmol solutions) were recorded on a Varian Cary 50 spectrophotometer using a quartz cell, in the range of 200-900 nm in CH₂Cl₂. NMR spectra were recorded in CDCl₃ solution (¹H, ¹³C and ³¹P) on a 300 MHz Bruker Avance II spectrometer and are referenced to the solvent residuals. The assignment of all the C and H resonances were confirmed by the 2D NMR techniques COSY, HSQC and HMBC. Archival NMR data is provided in Figures S6 – S9 in the SI.

Voltammetry. Cyclic voltammetry measurements were carried out at room temperature with a μ-Autolab (Type III, Metrohm-Eco Chemie) potentiostat/galvanostat. These experiments were performed using CH₃CN containing 0.10 M Bu₄NClO₄ (PTBA) as a supporting electrolyte and an electrochemical cell based on three electrodes: a 3 mm² glassy carbon working electrode, a platinum auxiliary electrode and an Ag/AgCl reference electrode in a Luggin capillary probe. Under these conditions, ferrocene (Fc) is oxidized at +0.375 V and the data are corrected to the Fc^{+/-} scale. Voltammograms were performed over multiple scan rates ranging from 0.1 – 2.0 V·s⁻¹. A full set of CV scans and their scan-rate dependency is provided in Figures S10 and S11 in the SI.

Synthesis. *Tris*-(3,5-di-*tert*-butylphenyl)phosphine, **1** [189756-42-1].⁴ A solution of 5.0 g (18.6 mmol) of 1-bromo-3,5-di-*tert*-butylbenzene in 18 mL of dry THF in a 250 mL flask equipped with a side-arm stopcock was cooled to -78 °C for 10 min with stirring. Then 13.2 mL (19.5 mmol) of nBuLi (1.6 M in hexane) was added during 10 min. Thereafter, 0.540 mL (6.2 mmol) of PCl₃ was added over a further 10 min. The resulting mixture was warmed to 0°C and then stirred for 30 min. After removing all volatiles to a vacuum trap, the residue was quenched with a solution of 10 mL of H₂O and mL 1M cH₂SO₄ which had previously been degassed by boiling under N₂, followed by 2 x 20 mL of CH₂Cl₂ which had been deoxygenated by sparging with N₂. The organic phase (CH₂Cl₂ + phosphine) was transferred by canula to a clean flask containing anhydrous Na₂SO₄, the dried solution underwent a second canula transfer and was evaporated to leave 3.13 g of a white powder (yield: 84.4%). ¹H NMR (300.13 MHz, CDCl₃): δ H₂ 1.21 (s, 54H, -C(CH₃)₃); H₁ 7.06 (d, 6H, J_{H-P} = 9.0 Hz); H₃ 7.34 (s, 3H, -CH) (lit. δ: 1.22, 7.08, 7.36), in good agreement with the literature values.⁴ {¹H}-¹³C NMR (100.61 MHz, CDCl₃): 31.63 (s, ^tBu_{Me}), 35.14 (s, ^tBu_c), 122.42 (s, C_{para}), 128.18 (d, ²J_{CP} = 19 Hz, C_{ortho}), 137.25 (d, ¹J_{CP} = 9 Hz, C_{ipso}), δ 150.58 (d, ³J_{CP} = 6.4 Hz, C_{meta}) (lit. δ: 31.36, 34.83, 122.19, 127.94).⁴ {¹H}-³¹P NMR (121.49 MHz, CDCl₃): δ -1.30. IR (Diamond ATR, v, cm⁻¹): 2951 s, 2897 m, 2867 m, 1578 m, 1472 m, 1418 m, 1388 m, 1365 s, 1286 w, 1239 s, 1197 w, 1124 m, 1016 w, 932 w, 901 m, 872 s, 781 w, 712 us, 583 m, 523 w, 475 m, 421 m (lit.: KBr 2950, 1575, 1475 cm⁻¹).⁴ For information on purification by recrystallization, see the SI.

Tris-(3,5-di-*tert*-butylphenyl)phosphine oxide monohydrate **5**. Leftovers of *tris*-(3,5-di-*tert*-butylphenyl)phosphine from various recrystallization attempts were placed in a 50 mL RB flask and dissolved in 20 mL of acetone. Thin-layer chromatography (elution: 95% hexanes; 5% ethyl acetate) was taken before reaction. Then the solution was heating with stirring to reflux and 4% aqueous H₂O₂ (0.7 mL of 30% H₂O₂ diluted with 5mL of H₂O) was added dropwise. Further TLC monitoring indicated reaction completion after 1 H. Crystals formed on cooling to RT and were filtered, taken up in 10 mL of CH₂Cl₂ and dried over anhydrous Na₂SO₄. After filtering and evaporation, the residue was recrystallized from 2 mL of boiling *n*-heptane. Cooling to -30°C afforded colourless crystals of a hydrate C₄₂H₆₃PO·nH₂O. 0.279 g. MP: 180-189 °C. Calc. for C₄₂H₆₃PO·0.35H₂O (best fit to residual water content; see Crystallography): C, 81.20; H, 10.34%. Found: C, 80.88; H, 9.96%. ¹H NMR (300.13 MHz, CDCl₃): δ H₁ 1.26 (s, 54H, -C (CH₃)₃); H₁ 7.46 (dd, 6H, J_{H-P} = 10.8 Hz);

H3 7.55 (t, 3H, -CH, $J_{H-H} = 1.8$ Hz) (lit. δ: 1.26, 7.48, 7.59).⁶ ^1H - ^{13}C NMR (75.48 MHz, CDCl₃): δ C_e 31.33 (s, -(CH₃)₃); C_d 35.01 (s, -C(CH₃)₃), C_f 125.55 (d, $^4J_{C-P} = 7$ Hz); C_b 126.45 (d, $^2J_{C-P} = 11$ Hz); C_a 132.18 (d, $^1J_{C-P} = 103$ Hz); C_c 150.61 (d, $^3J_{C-C} = 12$ Hz) (lit. δ: 31.3, 35.0, 126.2, 126.6, 130.2, 150.9).⁶ ^{31}P NMR (121.49 MHz, CDCl₃): δ +35.00. UV (dichloromethane, 5 × 10⁻⁵ mol·L⁻¹): λ_{max} = 272 nm (ε = 3128), λ_{max} = 280 nm (ε = 2938). IR (Diamond ATR, ν, cm⁻¹): 2954 s, 2903 w, 2857 w, 1587 w, 1479 m, 1425 m, 1388 w, 1359 m, 1239 m, 1184 m, 1148 s, 1016 w, 925 w, 896 w, 884 w, 871 m, 789 s, 711 s, 608 us, 529 s, 485 us, 448 s, 387 w.

Tris-(3,5-di-tert-butylphenyl)phosphine sulfide **6**. A 25 mL RB flask was charged with 300 mg (0.50 mmol) of **1** and 50 mg (0.19 mmol) of S₈ in 5 mL of *m*-xylene. The solution was refluxed with stirring for 2 H with periodic monitoring by TLC (hexanes). When all **1** was consumed, the cooled solution was evaporated to dryness. The residue was recrystallized from 6 mL of *n*-heptane at the boil, affording white crystals on cooling to RT which were filtered and dried (0.172 g, 57.3% yield). MP 240–250 °C. Calc. for C₄₂H₆₃PS: C, 79.94; H, 10.06; S, 5.08 %. Found: C, 80.18; H, 9.79; S, 4.90 %. ^1H NMR (300.13 MHz, CDCl₃): δ H₂ 1.24 (s, 54H, -C(CH₃)₃); H₁ 7.46 (dd, 6H, $J_{H-P} = 14,40$ Hz); H₃ 7.50 (t, 3H, -CH, $J_{H-H} = 1.8$ Hz). ^{13}C NMR (75.48 MHz, CDCl₃): δ C_e 31.29 (s, -(CH₃)₃); C_d 35.06 (s, -C(CH₃)₃), C_f 125.21 (d, $^4J_{C-P} = 3$ Hz); C_b 127.57 (d, $^2J_{C-P} = 11$ Hz); C_a 131.50 (d, $^1J_{C-P} = 76$ Hz); C_c 150.70 (d, $^3J_{P-C} = 12$ Hz). ^{31}P NMR (121.49 MHz, CDCl₃): δ +47.92. UV-vis (dichloromethane, 5 × 10⁻⁵ mol·L⁻¹): λ₁ = 282 nm (ε = 8216), λ₂ = 274 nm (ε = 10158). IR (Diamond ATR, ν, cm⁻¹): 2955 m, 2897 w, 2868 w, 1591 w, 1474 m, 1422 m, 1393 m, 1358 m, 1247 m, 1195 w, 1139 m, 1129 s, 1021 w, 922 w, 896 w, 882 w, 857 w, 780 m, 707 s, 661 us, 588 m, 527 m, 480 us, 437 m.

Tris-(3,5-di-tert-butylphenyl)phosphine selenide **7**. A 25 mL RB flask was charged with 300 mg (0.50 mmol) of **1** and 210 mg (2.66 mmol) of gray Se in 5 mL of *m*-xylene. The solution was refluxed with stirring for 2 H with periodic monitoring by TLC (95% hexanes/5% ethyl acetate). The solution was then cooled to RT and filtered through a plug of Celite™ to remove excess Se. The residue was evaporated and then recrystallized from 6 mL of *n*-heptane which on cooling to RT afforded white crystals (0.1 g, 37% yield). MP 274–278 °C. Calc. for C₄₂H₆₃PSe: C, 74.42; H, 9.37%. Found: C, 73.96; H, 8.91%. ^1H NMR (300.13 MHz, CDCl₃): δ H₂ 1.4 (s, 54H, -C(CH₃)₃); H₁ 7.44 (dd, 6H, $J_{H-P} = 14$ Hz); H₃ 7.50 (t, 3H, -CH, $J_{H-H} = 1.5$ Hz). ^{13}C NMR (75.48 MHz, CDCl₃): δ C_e 31.29 (s, -(CH₃)₃); C_d 35.06 (s, -C(CH₃)₃), C_f 125.21 (d, $^4J_{C-P} = 3$ Hz); C_b 126.95 (d, $^2J_{C-P} = 11$ Hz); C_a 131.5 (d, $^1J_{C-P} = 76$ Hz); C_c 150.70 (d, $^3J_{P-C} = 12$ Hz). ^{31}P NMR (121.49 MHz, CDCl₃): δ +39.54 ($J_{P-Se} = 719$ Hz). Lit value δ +37.4 ($J_{P-Se} = 714.0$ Hz).³ UV-vis (dichloromethane, 5 × 10⁻⁵ mol·L⁻¹): λ₁ = 273 nm (ε = 8960), λ₂ = 441 nm (ε = 566), λ₃ = 505 nm (ε = 398), λ₄ = 692 (ε = 226). IR (Diamond ATR, ν, cm⁻¹): 2955 s, 2902 w, 2862 w, 1586 w, 1468 m, 1416 m, 1393 w, 1358 s, 1247 s, 1195 w, 1130 s, 1019 w, 926 w, 898 w, 878 w, 859 w, 787 m, 774 w, 706 us, 607 us, 587 m, 528 s, 499 s, 479 us, 436 s, 389 w.

Crystallography. The structures of **1** and **5 – 7** were determined by single crystal X-ray crystallography at 100 K on a Rigaku-Oxford Diffraction SuperNova diffractometer equipped with a Pilatus P200 HPAD detector and using Cu $K\alpha$ radiation, $\lambda = 1.54184$ Å. Crystals were coated in Paratone™ oil, mounted on a MiTeGen loop and cooled to 100(1) K on the goniometer using the cold gas from an Oxford Cryostream 800. The images were integrated, the data processed and corrected for absorption using CrysAlisPro 1.171.38.43, solved with SHELXT,⁶¹ and refined using SHELXL-2014⁶² within the Olex2 suite of programs.⁶³ Only the structure of **6** was fairly straightforward with only some ^tBu rotational disorder to account for. Full details regarding the solution and refinement of these structures, including superlattice effects, are provided in the SI, along with tables of crystal and data collection parameters (Tables S1) and derived parameters (Table S2). Graphical output of the full structure of **1** is provided in Figure S1. Comparisons of the ‘flat’ and helical conformations in **1** with structures found in metal complexes and by computation are in Figure S2. A supercell refinement of **5** is depicted in Figure S3 and various space-filling shapes in Figures S4 and S5. Structures were visualized and

analyzed using Mercury CSD.⁶⁴ The crystallographic data have been deposited at the Cambridge Crystallographic Data Centre as CCDC 1834017 – 1834020.

Acknowledgements

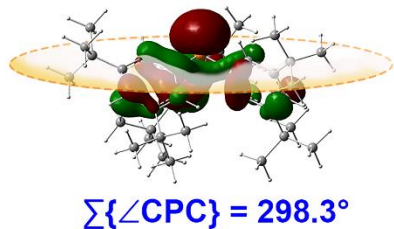
The authors thank the Brazilian agencies (CNPq PVE 401271/2014-5 and CAPES) and the NSERC-Canada (Discovery Grant to RTB) for generous financial support. We especially acknowledge the University of Lethbridge for purchasing the SuperNova X-ray diffractometer. We thank Dr. Eric Reinheimer of Rikagu Americas for providing significant assistance with the disorder models and data processing for some of the crystal structures.

- [1] M. Naruto, S. Saito, *Nat. Commun.* **2015**, 6:8140 (doi: 10.1038/ncomms9140).
- [2] B. Vulovic, A. P. Cinderella, D. A. Watson, *ACS Catal.* **2017**, 7, 8113-8117.
- [3] A. P. Cinderella, B. Vulovic, D. A. Watson, *J. Am. Chem. Soc.* **2017**, 139, 7741-7744.
- [4] K. Manabe, *Tetrahedron*, **1998**, 54, 14465-14476. The authors of ref. [3] have ascribed a name to **1**, "DREWphos". Whatever the merits are of trying to name compounds after lab employees, it seems unethical to ignore the right of discovery. We respectfully suggest it should be called MANABEphos.
- [5] M. Ullrich, A. J. Lough, D. W. Stephan, *Organometallics* **2010**, 29, 3647-3654.
- [6] M. Szigeti, Z. Dobi, T. Soós, *J. Org. Chem.* **2018**, 83, 2869-2874.
- [7] D. Gust, K. Mislow, *J. Am. Chem. Soc.* **1972**, 95, 1535-1547.
- [8] J. D. Andose, K. Mislow, *J. Am. Chem. Soc.* **1974**, 96, 2128-2167.
- [9] K. Mislow, *Acc. Chem. Res.* **1976**, 9, 26-33.
- [10] M. R. Kates, J. D. Andose, P. Finocchiaro, D. Gust, K. Mislow, *J. Am. Chem. Soc.* **1977**, 97, 1772-1778.
- [11] M. Landman, T. Levell, P. H. van Rooyen, J. Conradie, *J. Mol. Struct.* **2014**, 1065-1066, 29-38.
- [12] S. Rizzo, R. Cirilli, M. Pierini, *Chirality* **2014**, 26, 601-606.
- [13] B. Laleu, G. Bernardinelli, R. Chauvin, J. Lacour, *J. Org. Chem.* **2006**, 71, 7412-7416.
- [14] S. Sasaki, M. Yoshifuji, *Curr. Org. Chem.* **2007**, 11, 17-31.
- [15] T. Benincori, V. Bonometti, R. Cirilli, P. R. Mussini, A. Marchesi, M. Pierini, T. Pilati, S. Rizzo, F. Sannicola, *Chem. Eur. J.* **2013**, 19, 165-181.
- [16] C. Puigjaner, S. Vela, M. Font-Bardiac, J. J. Novoa, *CrystEngComm* **2014**, 16, 8214-8223.
- [17] L. Dubován, A. Pöllnitz, C. Silvestru, *Eur. J. Inorg. Chem.* **2016**, 1521–1527.
- [18] J. F. Costello, S. G. Davies, E. T. F. Gould, J. E. Thomson, *Dalton Trans.* **2015**, 44, 5451-5466.
- [19] J. Conradie, *Dalton Trans.* **2012**, 41, 10633-10642.
- [20] J. F. Costello, S. G. Davies, *J.C.S. Perkins Trans.* **1998**, 2, 1683-1689.
- [21] H. Brunner, R. Oeschey, B. Nuber, *Angew. Chem. Int. Ed. Engl.* **1994**, 33, 866-868.
- [22] N. D. D. Hill, R. T. Boeré, *Acta Crystallogr., Sect. E: Crystallogr. Commun.* **2018**, E74, 889–894.
- [23] U. Hengartner, D. Valentine, Jr., K. K. Johnson, M. E. Larscheid, F. Pigott, F. Scheidl, J. W. Scott, R. C. Sun, J. M. Townsend, T. H. Williams, *J. Org. Chem.* **1979**, 44, 3741-3747.
- [24] J. K. Romain, J. W. Ribblett, R. W. Byrn, R. D. Snyder, B. N. Storhoff, J. C. Huffman, *Organometallics* **2000**, 19, 2047-2050.
- [25] J. Bruckmann, C. Krüger, F. Lutz, *Z. Naturforsch.* **1995**, 50b, 351-360.
- [26] R. T. Boeré, A. M. Bond, S. Cronin, N. W. Duffy, P. Hazendonk, J. D. Masuda, K. Pollard, Kyle; T. L. Roemmele, P. Tran, Y. Zhang, *New J. Chem.* **2008**, 32, 214-231.
- [27] J. P. Bullock, A. M. Bond, R. T. Boeré, T. M. Gietz, T. L. Roemmele, S. D. Seagrave, J. D. Masuda, M. Parvez, *J. Am. Chem. Soc.* **2013**, 135, 11205-11215.
- [28] S. Sasaki, K. Sutoh, F. Murakami, M. Yoshifuji, *J. Am. Chem. Soc.* **2003**, 124, 14830-14831.
- [29] J. F. Blount, D. Camp, R. D. Hart, P. C. Healy, B. W. Skelton, A. H. White, *Aust. J. Chem.* **1994**, 47, 1631-1639.

- [30] M. Alcarazo, *Acc. Chem. Res.* **2016**, *49*, 1797-1805.
- [31] E. Haldón, Á. Kozma, H. Tinnermann, L. Gu, R. Goddard, M. Alcarazo, *Dalton Trans.* **2016**, *45*, 1872-1876.
- [32] H. Tinnermann, C. Wille, M. Alcarazo, *Angew. Chem. Int. Ed.* **2014**, *53*, 8732 –8736.
- [33] R. T. Boeré, Y. Zhang, *J. Organomet. Chem.* **2005**, *690*, 2651-2657.
- [34] T. Iwai, M. Sawamura, *Bull. Chem. Soc. Jpn.* **2014**, *87*, 1147–1160.
- [35] H. Ohta, M. Tokunaga, Y. Obora, T. Iwai, *Org. Lett.* **2007**, *9*, 89-92.
- [36] Y. Ohzu, K. Goto, H. Sato, T. Kawashima, *J. Organomet. Chem.* **2005**, *690*, 4175-4183.
- [37] Y. Ohzu, K. Goto, T. Kawashima, *Angew. Chem. Int. Ed. Engl.* **2003**, *42*, 5714-5717.
- [38] K. M. Steed, J. W. Steed, *Chem. Rev.* **2015**, *115*, 2895-2933.
- [39] C. P. Brock, *Acta Crystallogr., Sect. B: Struct. Sci.* **2016**, *72*, 807–821.
- [40] F. H. Allen, *Acta Crystallogr., Sect. B: Struct. Sci.* **2002**, *58*, 380–388.
- [41] R. S. Cahn, C. Ingold, V. Prelog, *Angew. Chem., Int. Ed. Engl.* **1966**, *5*, 385-415.
- [42] Centrosymmetry over the whole unit cell ensures that there are six of each *M* and *P* enantiomer in the racemic crystal.
- [43] The Durham University Z' database is now located at <http://zprime.co.uk/>.
- [44] P. G. Jessop, M. M. Olmstead, C. D. Ablan, M. Grabenauer, D. Sheppard, C. A. Eckert, C. L. Liotta, *Inorg. Chem.* **2002**, *41*, 3463-3468.
- [45] O. bin Shawkataly, M. A. A. Pankhi, M. I. Mohamed-Ibrahim, M. R. Hamdan, H.-K. Fun, *Acta Crystallogr., Sect. E: Struct. Rep. Online* **2009**, *65*, o1080.
- [46] J. A. S. Howell, N. Fey, J. D. Lovatt, P. C. Yates, P. McArdle, D. Cunningham, E. Sadeh, H. E. Gottlieb, Z. Goldschmidt, M. B. Hursthouse, M. E. Light, *J. Chem. Soc., Dalton Trans.* **1999**, 3015-3028.
- [47] M. Culcasi, Y. Berchadsky, G. Gronchi, P. Tordo, *J. Org. Chem.* **1991**, *56*, 3537-3542.
- [48] J. E. Leffler, E. Grunwald, *Rates and Equilibria of Organic Reactions*, Wiley, 1963 (Dover reprint).
- [49] U. Beckmann, D. Süslüyan, P. Kunz, *Phos. Sulf. Sil. Rel. Elem.* **2011**, *186*, 2061–2070.
- [50] R. T. Boeré, Y. Zhang, *Acta Cryst., Sect. C: Cryst. Struct. Comm.* **2013**, *69*, 1051-1054.
- [51] D. J. Brauer, M. Hingst, K. W. Kottsieper, C. Like, T. Nickel, M. Tepper, O. Stelzer, W. S. Sheldrick, *J. Organomet. Chem.* **2002**, *645*, 14-26.
- [52] An earlier definition of the "fold back" angle α was a useful tool to describe pyramidality in the era of using Z-matrices to describe geometries – see ref. 47. An average value for α can be defined from our pyramidality index: $\alpha = \cos^{-1}[\{\sin(\angle CPC)/6\}/\cos 30^\circ]$.
- [53] J. A. Thomas, T. A. Hamor, *Acta Crystallogr., Sect. C: Cryst. Struct. Commun.* **1993**, *49*, 355-357.
- [54] T. Schulz, K. Meindl, D. Leusser, D. Stern, J. Graf, C. Michaelsen, M. Ruf, G. M. Sheldrick, D. Stalke, *J. Appl. Crystallogr.* **2009**, *42*, 885-891.
- [55] P. W. Codding, K. A. Kerr, *Acta Crystallogr., Sect. B: Struct. Crystallogr. Cryst. Chem.* **1979**, *35*, 1261-1263.
- [56] S. Grimme, J. Antony, S. Ehrlich, H. Krieg, *J. Chem. Phys.* **2010**, *132*, 154104.
- [57] C. Bannwarth, S. Grimme, *J. Chem. Phys.*, **2017**, *147*, 034112.
- [58] G. Bistoni, A. A. Auer, F. Neese, *Chem. Eur. J.*, **2017**, *23*, 865-873.
- [59] S. Rösel, C. Balestrieri, P. R. Schreiner, *Chem. Sci.*, **2017**, *8*, 405-410.
- [60] C. Esterhuysen, A. Heßelmann, T. Clark, *Chem. Phys. Chem.*, **2017**, *18*, 772-784.
- [61] G. M. Sheldrick, *Acta Crystallogr., Sect. A: Foundat. Adv.* **2015**, *71*, 3-8.
- [62] G. M. Sheldrick, *Acta Crystallogr., Sect. C: Struct. Chem.* **2015**, *71*, 3-8.
- [63] O. V. Dolomanov, L. J. Bourhis, R. J. Gildea, J. A. K. Howard, H. Puschmann, *J. Appl. Cryst.* **2009**, *42*, 339 -341.

- [64] C. F. Macrae, I. J. Bruno, J. A. Chisholm, P. R. Edgington, P. McCabe, E. Pidcock, L. Rodriguez-Monge, R. Taylor, J. van de Streek, P. A. Wood, *J. Appl. Cryst.* **2008**, *41*, 466-470.

Graphical Abstract and TOC Text



MANABEphos, valued as a supporting ligand because of the distal steric bulk from the *exo*-oriented *tert*butyl groups, is also rendered more pyramidal than PPh_3 through London dispersion forces on and between the *endo*-substituents, which results in a raised HOMO energy and reduced basicity

Supporting Information

<u>Table of Contents</u>	<u>Page No.</u>
<i>Crystallography: further details</i>	S2
Table S1 Crystal, structure determination and refinement parameters	S2
Table S2 Selected bond lengths [Å] and angles [°] in the crystal structure of 1 and 5 – 7	S4
Figure S1 Further displacement ellipsoids plots of 1	S6
Figure S2 (a) Flat conformation adopted by 1 ; (b) Overlay of DFT and P300 structures in 1	S7
Figure S3 Displacement ellipsoids plot of the super-cell of 5	S7
Figure S4 Space-filling representations of the water-bridged dimers of 5	S8
Figure S5 Space-filling plots of 1 and 5 – 7	S8
Table S3 Hydrogen bonded inter-oxygen distances (Å) in 5 and related analogues	S9
<i>Archival NMR spectra</i>	
Figure S6 ^1H -NMR and ^{31}P spectra of 1 in CDCl_3 (300 MHz)	S10
Figure S7 ^1H -NMR and ^{31}P spectra of 5 in CDCl_3 (300 MHz)	S10
Figure S8 ^1H -NMR and ^{31}P spectra of 6 in CDCl_3 (300 MHz)	S11
Figure S9 ^1H -NMR and ^{31}P spectra of 7 in CDCl_3 (300 MHz)	S11
<i>Archival voltammetric data</i>	
Figure S10 Cyclic voltammetric data for phosphines 1 – 4 and scan-rate dependence	S12
Figure S11 Peak current variation for 1 – 4 with root square of scanning rate	S13
Figure S12 Correlation between E_p^a and estimated Hammett σ^+ parameters	S13
<i>Conformations in pyramidal propeller molecules like 1</i>	
Figure S13 Perspective drawing of (a) the <i>P</i> and <i>M</i> conformers, and (b) four 'flip' processes	S14
<i>DFT Calculations and archival computed geometries</i>	S15
<i>References for the Supporting Information</i>	S28

Table S1. Crystal, structure determination and refinement parameters

Parameter	1	5	6	7
Empirical formula	C ₄₂ H ₆₃ P	C ₄₂ H ₆₃ OP·0.8H ₂ O	C ₄₂ H ₆₃ PS	C ₄₂ H ₆₃ PSe
Formula weight	598.89	629.34	630.95	677.85
Temperature/K	99.9(2)	99.99(17)	100.00(10)	99.99(14)
Crystal system	monoclinic	triclinic	monoclinic	monoclinic
Space group	P ₂ ₁ /c	P ₁	P ₂ ₁ /c	P ₂ ₁ /c
a/Å	33.5426(3)	14.5038(2)	10.37504(9)	10.31240(10)
b/Å	10.06131(11)	16.8369(2)	19.11982(16)	19.3690(3)
c/Å	46.2696(5)	18.8775(2)	20.46184(16)	20.3821(3)
α/°	90	68.1500(10)		
β/°	93.3735(9)	72.7510(10)	91.3953(7)	90.5170(10)
γ/°	90	89.9500(10)		
Volume/Å ³	15588.1(3)	4054.98(9)	4057.79(6)	4070.97(10)
Z	16	4	4	4
Z'	4	2	1	1
ρ _{calc} g/cm ³	1.021	1.037	1.033	1.106
μ/mm ⁻¹	0.790	0.819	1.249	1.788
F(000)	5280	1392	1384	1456
Crystal size/mm ³	0.15 × 0.12 × 0.03	0.339 × 0.089 × 0.035	0.28 × 0.18 × 0.13	0.07 × 0.06 × 0.05
Radiation		CuKα (λ = 1.54184)		
2Θ range for data collection/°	6.7 to 155.122 -41 ≤ h ≤ 42, -6 ≤ k ≤ 12, -57 ≤ l ≤ 58	6.43 to 155.474 -18 ≤ h ≤ 18 -21 ≤ k ≤ 21 -23 ≤ l ≤ 23	8.526 to 155.128 -13 ≤ h ≤ 11 -23 ≤ k ≤ 23 -24 ≤ l ≤ 25	8.564 to 159.654 -13 ≤ h ≤ 13 -24 ≤ k ≤ 24 -26 ≤ l ≤ 25
Index ranges				
Reflections collected	98894	162605	40872	64116
Independent reflections	32038	17081	8443	8813
R _{int} =, R _{sigma} =	0.0381, 0.0401	0.0392, 0.0172	0.0382, 0.0257	0.0566, 0.0305
Completeness to theta = 67.684°	99.7 %		98.40	
Data/restraints/parameters	32038/1620/182517081/1146/1104		8443/426/477	8813/345/424
Goodness-of-fit on F ²	1.014	1.035	1.035	1.103
Final R ₁ [>2σ]	0.0562	0.0613	0.0636	0.0747
wR ₂ (all data)	0.1452	0.1618	0.1755	0.1895
Largest diff. peak/hole / e Å ⁻³	0.73/-0.39	0.89/-0.52	1.01/-0.69	1.04/-0.92

Crystallography: further details. The crystal structure of **1** proved challenging. In all, datasets from four crystals were obtained. The first crystal was obtained from recrystallization in 99% ethanol in which the compound is extremely soluble, so that the concentration in hot solvent is very high. This evidently reduces the ability of crystallization to differentiate the neutral phosphine from phosphine oxide, the presence of which in the recrystallization mixture was confirmed by ³¹P NMR. This structure, which is included as Figure S1a, contains significant residual peaks in difference maps consistent with oxygen attached to phosphorus. The refined model (ESI) fit about 12% oxide at the P1 molecule and smaller amounts at the other sites, for an average content of 4% oxide in the unit cell. The second and third crystals were grown from a 4:1 methanol/ethanol solvent mixture in which the concentration in hot solvent is about 17 times lower.

One of these crystals showed no significant residual peaks attributable to oxide but was too small a crystal to obtain redundant data in reasonable time, the other which is the reported structure has a largest peak, also found at P1, with an electron density of only $0.79 \text{ e}\cdot\text{\AA}^{-3}$, which barely exceeds the intensity expected for the non-bonded electron density. A fourth crystal was obtained from vacuum sublimation in a tube furnace. It was also small but showed the same unit cell as the crystals grown from solution.

It may be significant that in each case, the highest residual peak for oxygen in the asymmetric unit is always found on the 'flat' molecule, i.e. the one with P1 as the phosphine label (Figure S1a).

During refinement, six of the 24 independent ^tBu groups show sufficiently large evidence of rotational disorder to have been refined, each using an independent two-part model with the occupancies of the major components refining to 0.76 (C11), 0.69 (C47), 0.77 (C131), 0.54 (C207), 0.82 (C327) and 0.77 (C331) occupancies (central atom of affected ^tBu group identified). Small residuals indicating further rotational disorders were below the threshold for beneficial disorder modelling (the number of additional parameters outweighed the benefit of improved refinement). After considerable effort, a very acceptable structure model for **1** was achieved.

Crystals for **5** suitable for X-ray diffraction were obtained from acetone/water but a structure determination indicated the presence of bridging water molecules in the asymmetric unit with $Z' = 2$. Further chemical drying of the sample followed by recrystallization from hot *n*-heptane returned the *same* crystal habit. Water oxygen occupancy refinement indicated that this second set of crystals contained proportionately more water and somewhat less disorder than the first data set. The reported structure is from the crystal obtained from heptane. The refined model is badly disordered in (i) the location of water oxygen atoms (modelled by anisotropic refinement of a single site), (ii) ^tBu rotational disorder (C31, C111, C127 and C147 central atoms) and (iii) a whole aryl ring positional shift (C41 > C46 with attached ^tBu groups). Careful inspection of the diffraction intensities using the Ewald Explorer functionality within CrysAlisPro, release 38.43, showed weak spots at $a^*/2$. When indexed, this supercell with doubled volume (16.8620(3), 18.9104(4), 28.9785(5) \AA , 107.1323(17), 90.0015(14), 111.9750(17) $^\circ$ solved successfully as a $Z' = 4$ structure containing the two $\text{Ar}_3\text{P}=\text{O}-\{\text{H}_2\text{O}\}_2\text{O}=\text{PAr}_3$ dimers found as centrosymmetric dimers in the smaller cell as explicit molecules with only approximate centrosymmetry (Figure S3). However, refinement of the super-cell model stalled at $R_1 = 0.0814$ and in the end the model based on the smaller cell was judged to be the best attainable from this data. A representation of the asymmetric unit from the supercell is given in Figure S2. In all the models, the water bridging ($\text{P}=\text{O})_1$ with its symmetry partner has higher refined occupancy than that bridging ($\text{P}=\text{O})_{100}$. Perhaps significantly, the $\text{P}=\text{O}$ separation for the dimer with less water, $\text{O}100\cdots\text{O}100' = 5.274(2)$, is greater than for that with more water, $\text{O}1\cdots\text{O}1' = 4.680(2)$.

Crystals for **6** and **7** formed on cooling hot *n*-heptane solutions and were found to be isostructural. They differ primarily with regards to where the disorder occurs. In **6**, the C27 and C51 ^tBu groups are rotationally disordered (0.63 and 0.64 occupancies for the major components, respectively), whereas in **7** it is C47 and C51 (i.e. both on the same C41 > C46 phenyl ring) with 0.83 and 0.87 major occupancy factors. This structure also contains a whole molecule positional disorder for which only the Se and P atoms could be reliably located on the difference Fourier map with about 0.06 refined occupancy.

Selected bond lengths [\AA] and angles [$^\circ$] in the crystal structure of **1** and **5 – 7** are provided in Table S2.

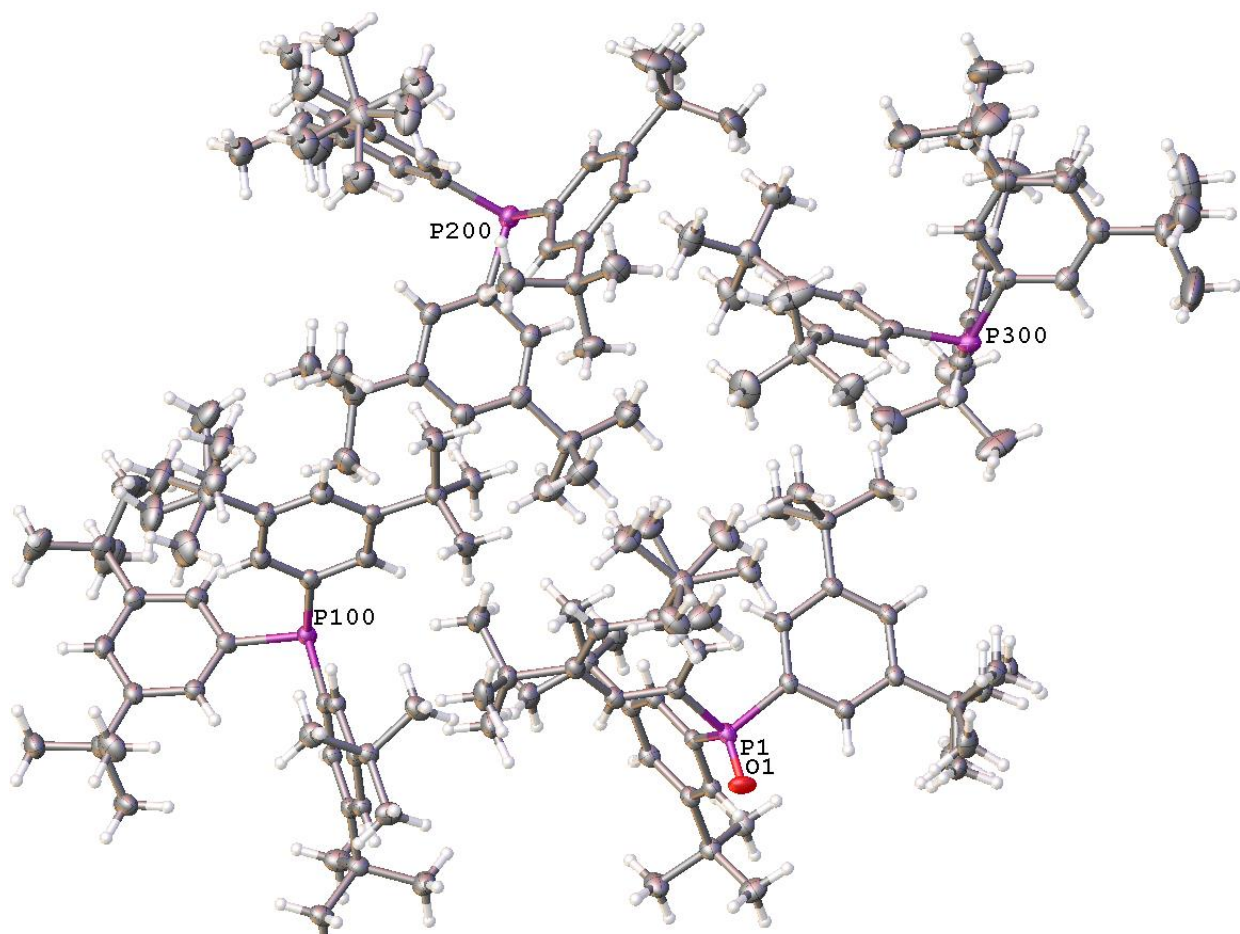
Table S2 Selected bond lengths [Å] and angles [°] in the crystal structure of **1** and **5 – 7**

1 Atoms	Dimensions	Atoms	Dimensions	Atoms	Dimensions
P(1)-C(1)	1.8164(19)	P(200)-C(241)	1.838(2)	C(2)-C(1)-C(6)	118.70(17)
P(1)-C(21)	1.8362(19)	C(201)-C(202)	1.389(3)	C(6)-C(1)-P(1)	120.25(14)
P(1)-C(41)	1.8420(18)	C(201)-C(206)	1.400(3)	C(101)-P(100)-C(121)	100.85(9)
C(1)-C(2)	1.400(3)	C(221)-C(222)	1.392(3)	C(101)-P(100)-C(141)	101.50(9)
C(1)-C(6)	1.403(3)	C(221)-C(226)	1.400(3)	C(121)-P(100)-C(141)	100.89(9)
C(21)-C(22)	1.398(3)	C(241)-C(242)	1.388(3)	C(102)-C(101)-P(100)	117.19(15)
C(21)-C(26)	1.387(3)	C(241)-C(246)	1.393(3)	C(106)-C(101)-P(100)	123.16(15)
C(41)-C(42)	1.393(3)	P(300)-C(301)	1.840(2)	C(106)-C(101)-C(102)	119.62(18)
C(41)-C(46)	1.390(3)	P(300)-C(321)	1.845(2)	C(201)-P(200)-C(221)	102.16(9)
P(100)-C(101)	1.829(2)	P(300)-C(341)	1.841(2)	C(201)-P(200)-C(241)	101.67(9)
P(100)-C(121)	1.841(2)	C(301)-C(302)	1.396(3)	C(241)-P(200)-C(221)	99.97(9)
P(100)-C(141)	1.846(2)	C(301)-C(306)	1.391(3)	C(202)-C(201)-P(200)	123.08(17)
C(101)-C(102)	1.402(3)	C(321)-C(322)	1.390(3)	C(202)-C(201)-C(206)	119.6(2)
C(101)-C(106)	1.387(3)	C(321)-C(326)	1.391(3)	C(206)-C(201)-P(200)	117.36(16)
C(121)-C(122)	1.403(3)	C(341)-C(342)	1.383(3)	C(301)-P(300)-C(321)	99.90(9)
C(121)-C(126)	1.388(3)	C(341)-C(346)	1.404(3)	C(301)-P(300)-C(341)	103.41(10)
C(141)-C(142)	1.411(3)	C(1)-P(1)-C(21)	104.63(8)	C(341)-P(300)-C(321)	100.04(9)
C(141)-C(146)	1.385(3)	C(1)-P(1)-C(41)	103.39(8)	C(302)-C(301)-P(300)	122.74(15)
P(200)-C(201)	1.834(2)	C(21)-P(1)-C(41)	100.51(8)	C(306)-C(301)-P(300)	118.24(15)
P(200)-C(221)	1.842(2)	C(2)-C(1)-P(1)	120.40(14)	C(306)-C(301)-C(302)	118.99(18)

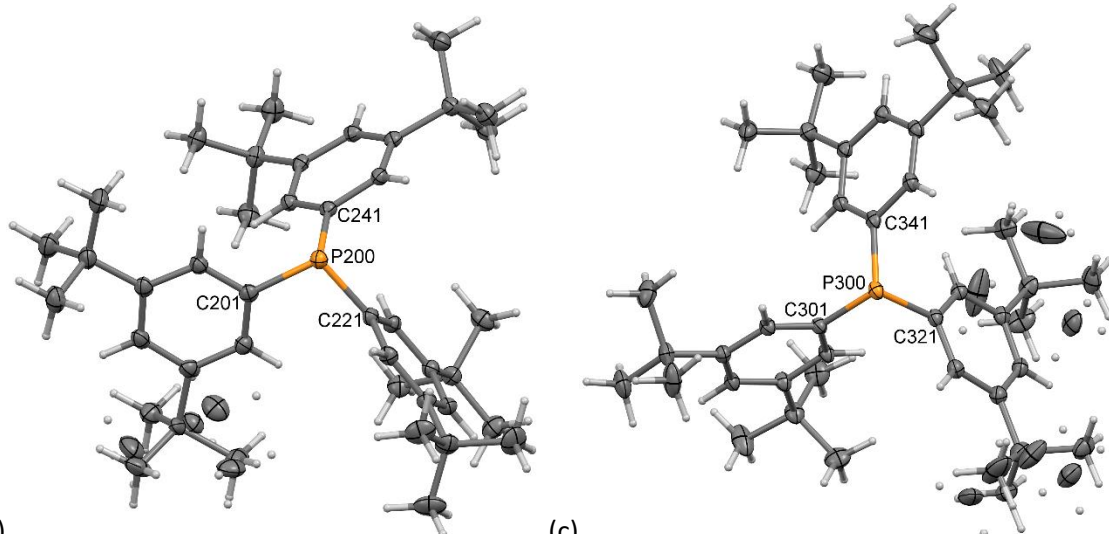
5 Atoms	Dimensions	Atoms	Dimensions	Atoms	Dimensions
P(1)-O(1)	1.4927(12)	C(101)-C(102)	1.394(2)	C(41)-P(1)-C(1)	105.4(3)
P(1)-C(1)	1.8017(16)	C(101)-C(106)	1.395(2)	C(41)-P(1)-C(21)	110.1(2)
P(1)-C(21)	1.8089(16)	C(1)-P(1)-C(21)	104.63(8)	C(2)-C(1)-P(1)	118.82(12)
P(1)-C(41)	1.752(7)	C(1)-P(1)-C(41)	103.39(8)	C(2)-C(1)-C(6)	120.34(15)
P(1)-C(41A)	1.934(13)	C(21)-P(1)-C(41)	100.51(8)	C(6)-C(1)-P(1)	120.73(13)
C(1)-C(2)	1.391(2)	C(2)-C(1)-P(1)	120.40(14)	O(100)-P(100)-C(101)	114.54(7)
C(1)-C(6)	1.394(2)	C(2)-C(1)-C(6)	118.70(17)	O(100)-P(100)-C(121)	112.49(7)
C(21)-C(22)	1.399(2)	C(6)-C(1)-P(1)	120.25(14)	O(100)-P(100)-C(141)	113.63(8)
C(21)-C(26)	1.391(2)	O(1)-P(1)-C(1)	112.61(8)	C(121)-P(100)-C(101)	105.00(7)
C(41)-C(42)	1.383(7)	O(1)-P(1)-C(21)	113.11(7)	C(141)-P(100)-C(101)	104.62(7)
C(41)-C(46)	1.390(6)	O(1)-P(1)-C(41)	109.9(2)	C(141)-P(100)-C(121)	105.69(7)
P(100)-O(100)	1.4915(12)	O(1)-P(1)-C(41A)	118.5(4)	C(102)-C(101)-P(100)	118.27(12)
P(100)-C(101)	1.8095(16)	C(1)-P(1)-C(21)	105.34(7)	C(102)-C(101)-C(106)	120.61(14)
P(100)-C(121)	1.8043(16)	C(1)-P(1)-C(41A)	106.8(5)	C(106)-C(101)-P(100)	120.98(12)
P(100)-C(141)	1.8021(18)	C(21)-P(1)-C(41A)	98.9(3)		

6 Atoms	Dimensions	Atoms	Dimensions	Atoms	Dimensions
S(1)-P(1)	1.9596(7)	C(41)-C(46)	1.391(3)	C(6)-C(1)-C(2)	120.07(19)
P(1)-C(1)	1.815(2)	C(1)-P(1)-S(1)	113.08(7)	C(22)-C(21)-P(1)	118.28(16)
P(1)-C(21)	1.819(2)	C(1)-P(1)-C(21)	104.35(9)	C(26)-C(21)-P(1)	121.49(15)
P(1)-C(41)	1.818(2)	C(1)-P(1)-C(41)	104.91(9)	C(26)-C(21)-C(22)	120.13(19)
C(1)-C(2)	1.395(3)	C(21)-P(1)-S(1)	114.11(7)	C(42)-C(41)-P(1)	118.61(15)
C(1)-C(6)	1.384(3)	C(41)-P(1)-S(1)	113.99(7)	C(46)-C(41)-P(1)	121.20(16)
C(21)-C(22)	1.398(3)	C(41)-P(1)-C(21)	105.43(9)	C(46)-C(41)-C(42)	120.18(19)
C(21)-C(26)	1.384(3)	C(2)-C(1)-P(1)	118.12(15)		
C(41)-C(42)	1.398(3)	C(6)-C(1)-P(1)	121.81(15)		

7 Atoms	Dimensions	Atoms	Dimensions	Atoms	Dimensions
Se(1)-P(1)	2.1154(10)	C(41)-C(46)	1.382(5)	C(42)-C(41)-P(1)	118.6(3)
P(1)-C(1)	1.825(4)	C(41)-P(1)-Se(1)	113.90(13)	C(22)-C(21)-P(1)	119.5(3)
P(1)-C(21)	1.820(4)	C(41)-P(1)-C(1)	104.61(17)	C(22)-C(21)-C(26)	120.3(4)
P(1)-C(41)	1.822(4)	C(21)-P(1)-Se(1)	113.66(13)	C(26)-C(21)-P(1)	120.2(3)
C(2)-C(1)	1.395(5)	C(21)-P(1)-C(41)	105.57(17)	C(2)-C(1)-P(1)	117.8(3)
C(1)-C(6)	1.380(5)	C(21)-P(1)-C(1)	105.23(18)	C(6)-C(1)-P(1)	121.5(3)
C(21)-C(22)	1.391(5)	C(1)-P(1)-Se(1)	112.98(13)	C(6)-C(1)-C(2)	120.8(4)
C(21)-C(26)	1.395(5)	C(46)-C(41)-P(1)	120.9(3)		
C(41)-C(42)	1.395(5)	C(46)-C(41)-C(42)	120.5(3)		



(a)



(b)

(c)

Figure S1. (a) Displacement ellipsoids plot showing the asymmetric unit of **1** as found in the crystal structure determination of the crystals grown from ethanol. There are four independent molecules labelled by their phosphorus atoms as P1, P100, P200 and P300. The approximately 12% refined occupancy for O1 represents the largest concentration of oxide in the lattice. Smaller residual peaks attributable to oxide co-crystallization are found for P100-300 (0.4 to $0.6 \text{ e}\cdot\text{\AA}^{-3}$). (b) A displacement ellipsoids plot (30% probability) for the P200 molecule in the reported structure of **1** and (c) the same for the P300 molecule.

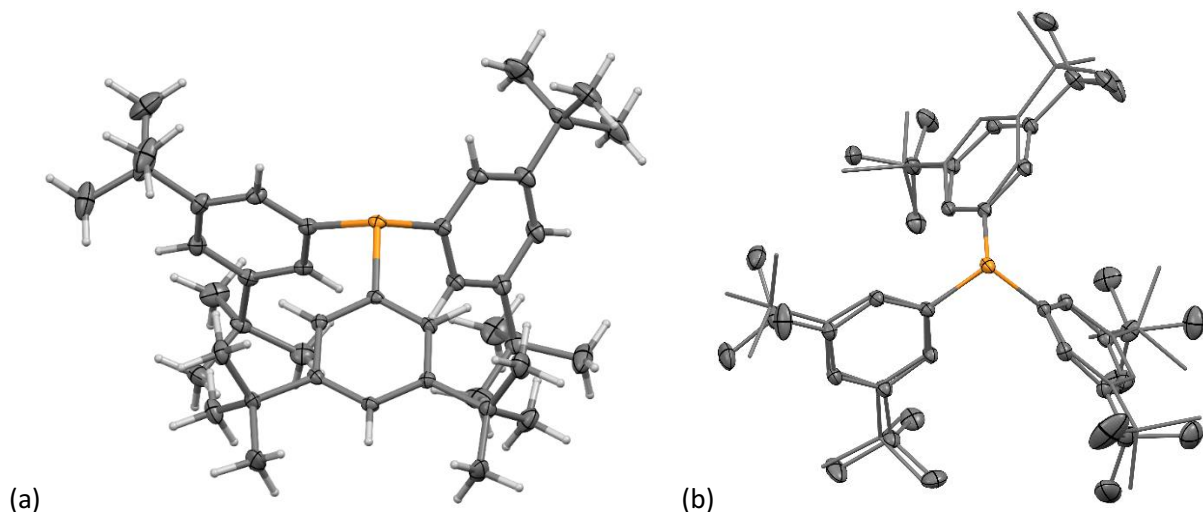


Figure S2. (a) 'Flat' conformation adopted by **1** in the centrosymmetric structure found in crystals of the palladium(II) iodide complex reported by Cinderella et al. (b) Overlay of the DFT minimized geometry of **1** with that found in the crystal structure for molecule P300.

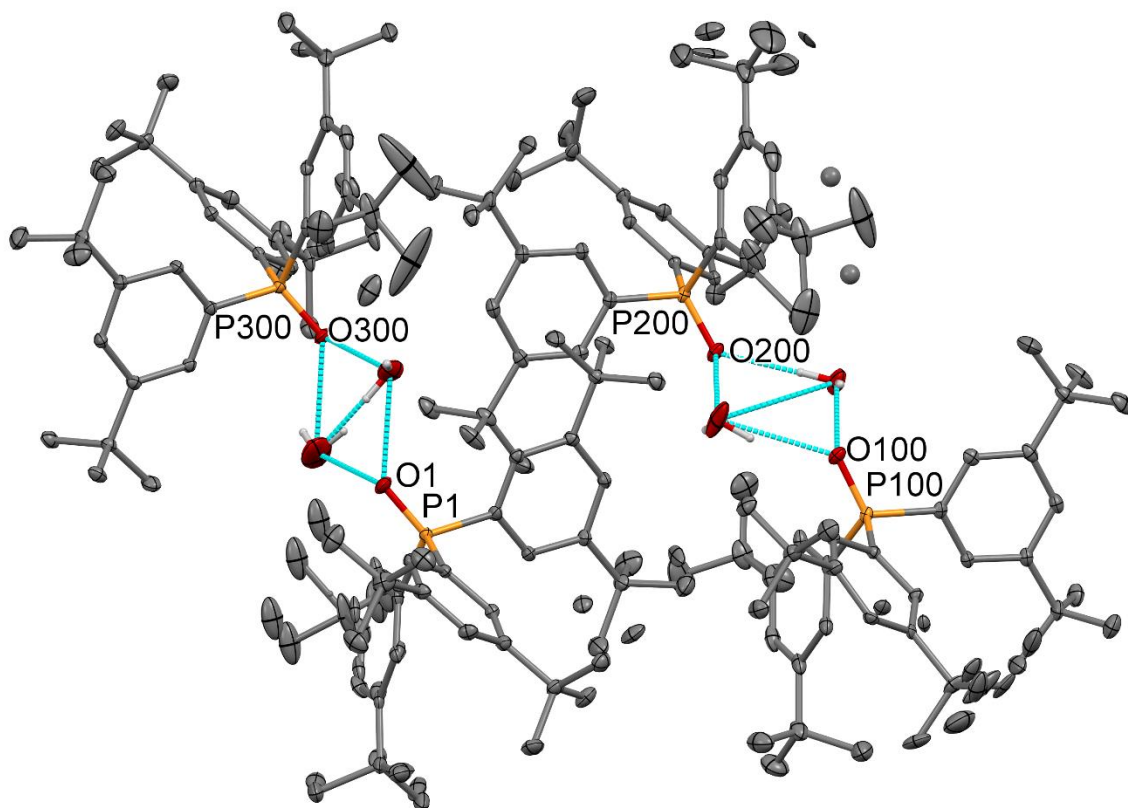
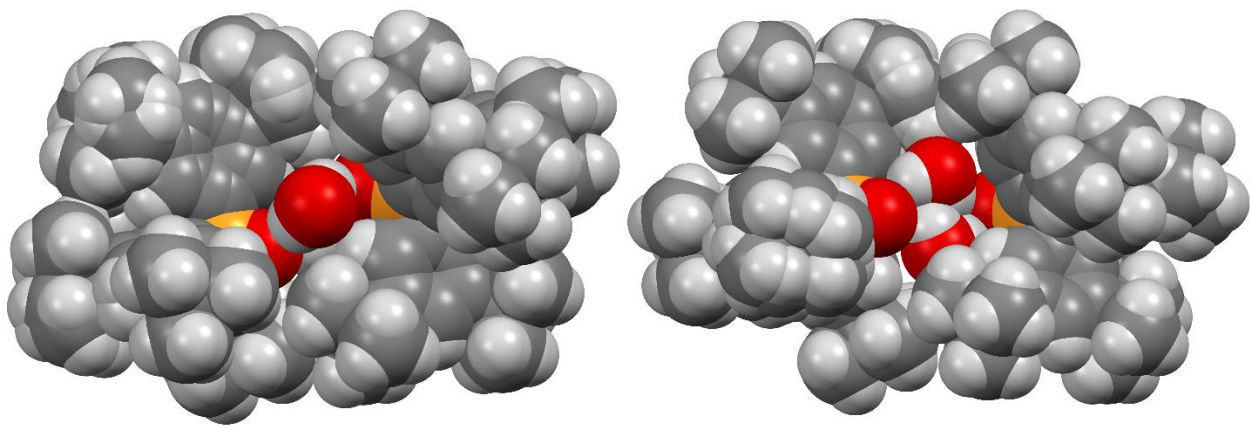


Figure S3. Displacement ellipsoids plot from a refinement of the super-cell in the crystal structure of **2** (see Experimental section for further details.)



(a)

(b)

Figure S4. Space-filling representations of the P1/O1 (a) and P100/O100 (b) water-bridged dimers found in the crystal structure of **2**.

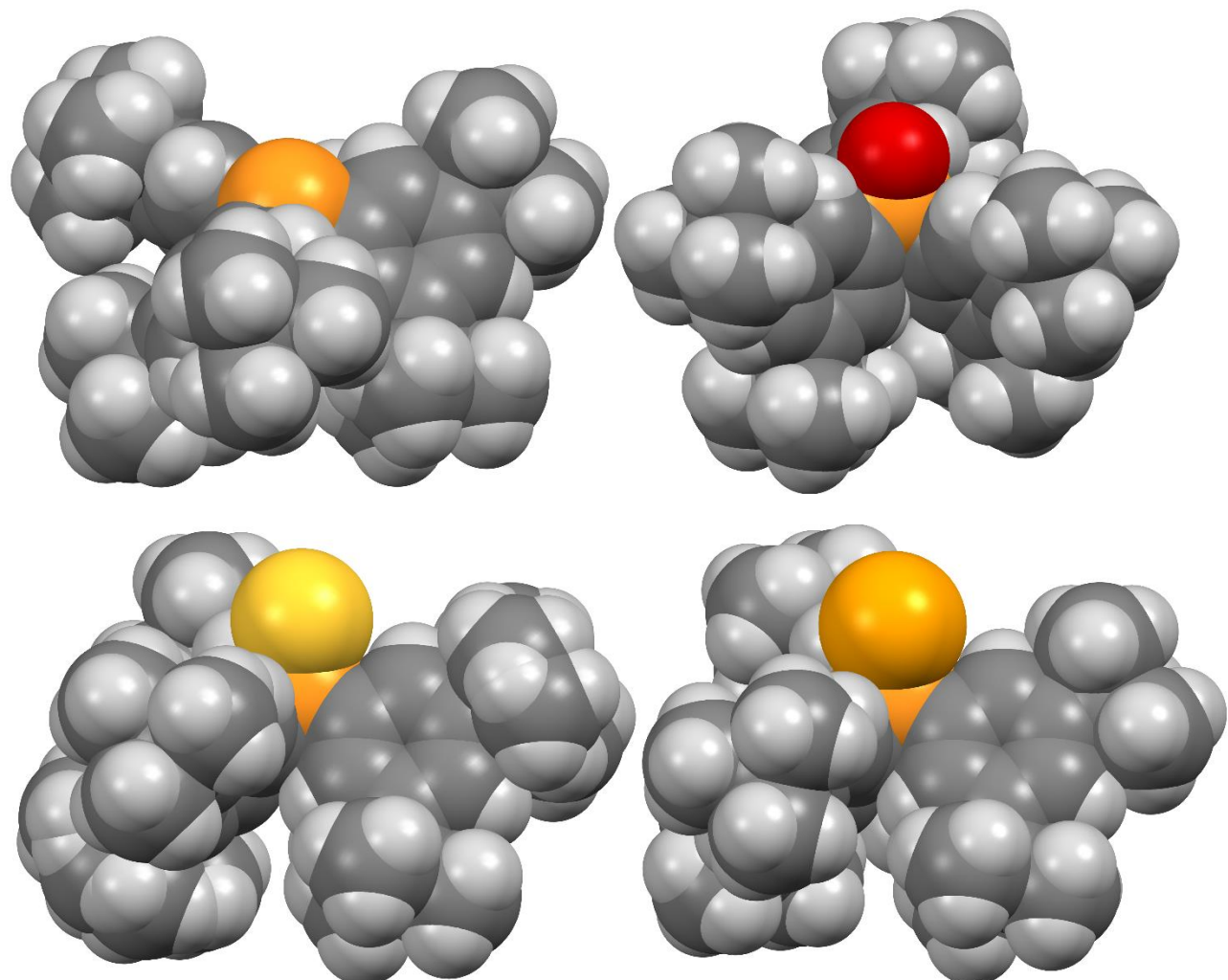


Figure S5. Space-filling plots of representative monomeric molecules in the series **1** and **5 – 7**.

Table S3. Hydrogen bonded donor-acceptor inter-oxygen distances (\AA) in **2** and 25 comparable structures

Refcode	Dist1	Dist2	Mean	Symmetry	Reference
VAGXEJ	2.683	2.677	2.680	-1	
XIBVAF	2.760	2.649	2.705	-1	
ABAYIN	2.908	2.671	2.790	-1	
VIGTOV	2.780	2.828	2.804	-1	
HUTNOZ	2.814	2.799	2.807	-1	
XOBPUA	2.777	2.853	2.815	-1	
XEZNEV	2.797, 2.813	2.839, 2.824	2.824	2(1)	
KEZQIR	2.807	2.858	2.833	-1	
UVAWOEF	2.822	2.864	2.843	-1	
BUHZEK	2.806	2.887	2.847	-1	
FAXHES	2.882	2.812	2.847	-1	
SISLIQ	2.897	2.801	2.849	-1	
EYINOP	2.843	2.860	2.852	-1	
GOYKEM	2.853	2.863	2.858	-1	
TIKJED	2.912	2.815	2.864	-1	
CUDYUV	2.868	2.861	2.865	-1	
XOFBUP	2.799	2.930	2.865	-1	
POCDEC	2.901	2.841	2.871	-1	
HATTUR	2.879	2.884	2.882	-1	
HATTUR01	2.881	2.895	2.888	-1	
RIZCEI	2.849	2.927	2.888	-1	
GIHVEY	2.855	2.923	2.889	-1	
NOYQEZ	2.890	2.894	2.892	-1	
HATTUR02	2.890	2.897	2.894	-1	
BUWYAV	2.883	2.919	2.901	-1	
2	2.861, 2.902	2.981, 3.065	2.952	-1	

Data taken from a search of the CSD (Version 5.39, November 2017).¹

Archival NMR Data

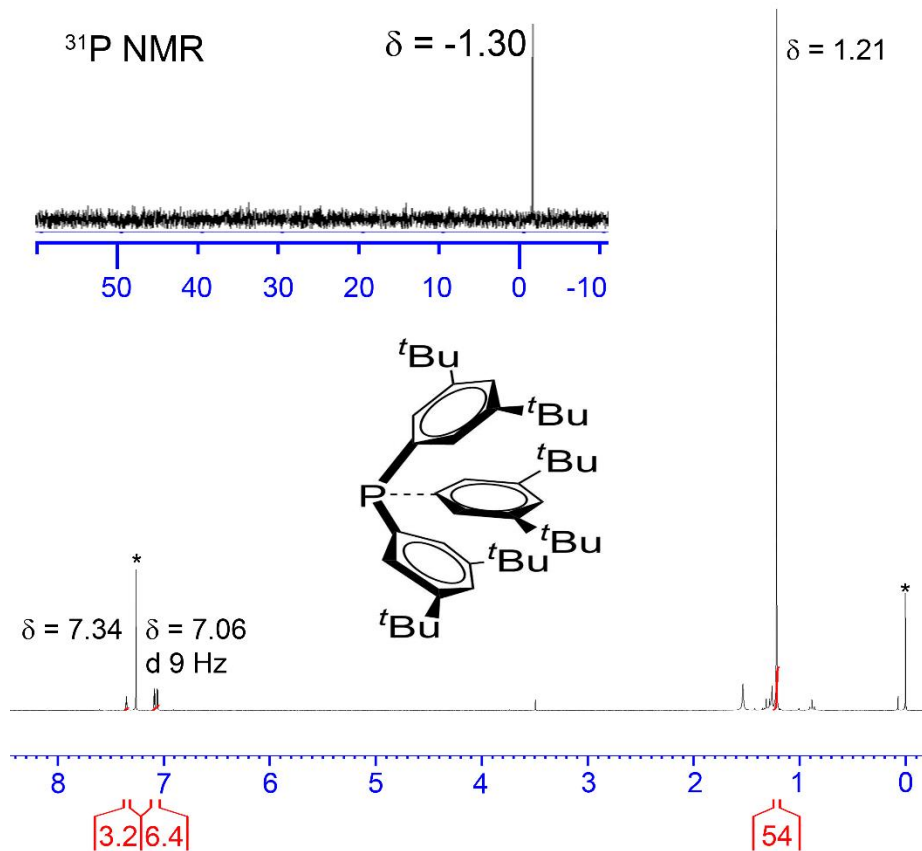


Figure S6 ¹H NMR spectrum of **1** in CDCl₃. Inset: ³¹P NMR spectrum of **1**.

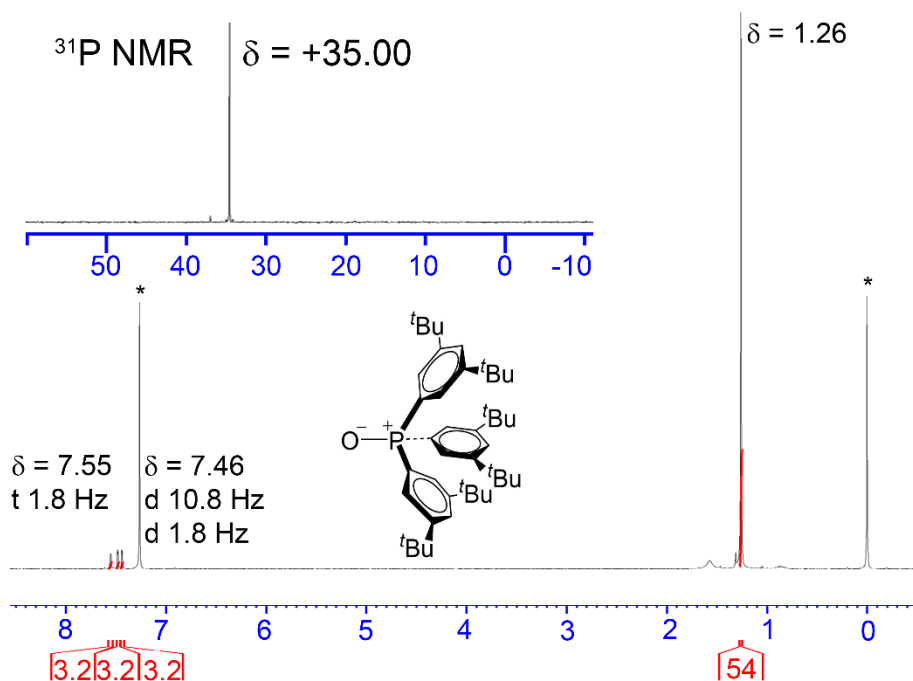


Figure S7 ¹H NMR spectrum of **5** in CDCl₃. Inset: ³¹P NMR spectrum of **5**.

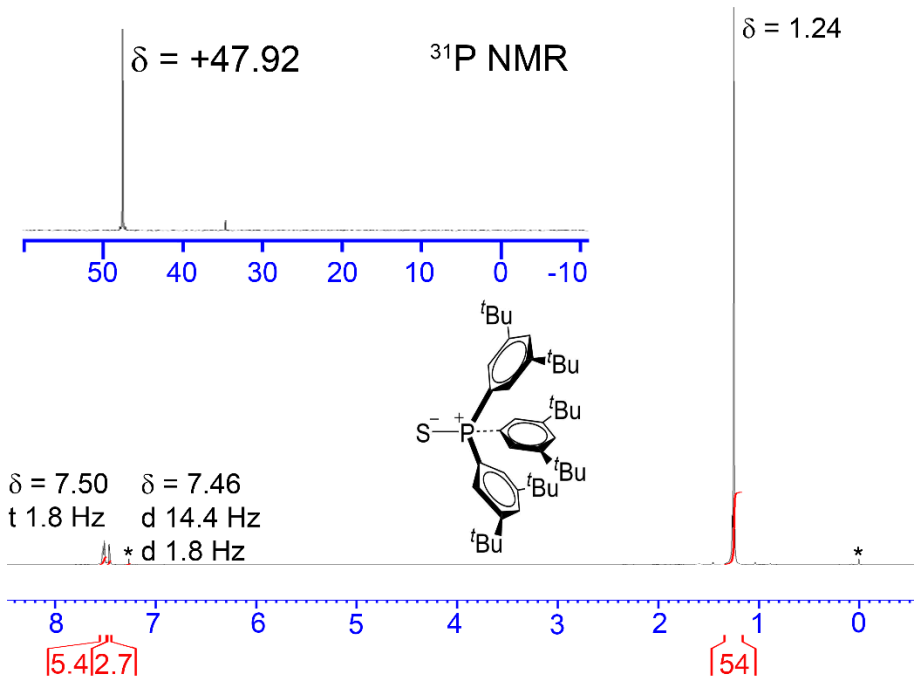


Figure S8 ${}^1\text{H}$ NMR spectrum of **6** in CDCl_3 . Inset: ${}^{31}\text{P}$ NMR spectrum of **6**.

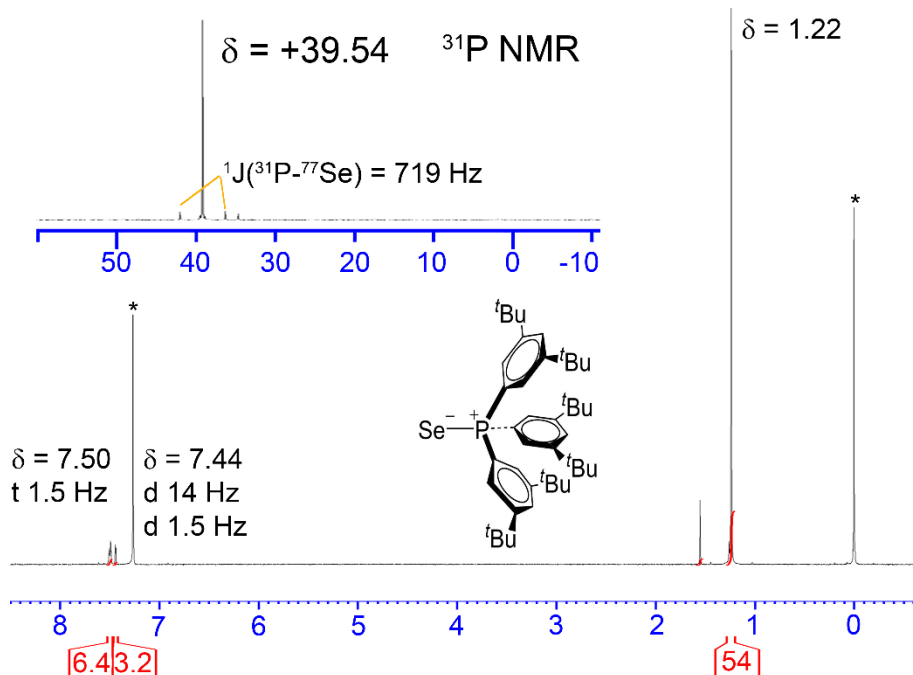


Figure S9 ${}^1\text{H}$ NMR spectrum of **7** in CDCl_3 . Inset: ${}^{31}\text{P}$ NMR spectrum of **7**.

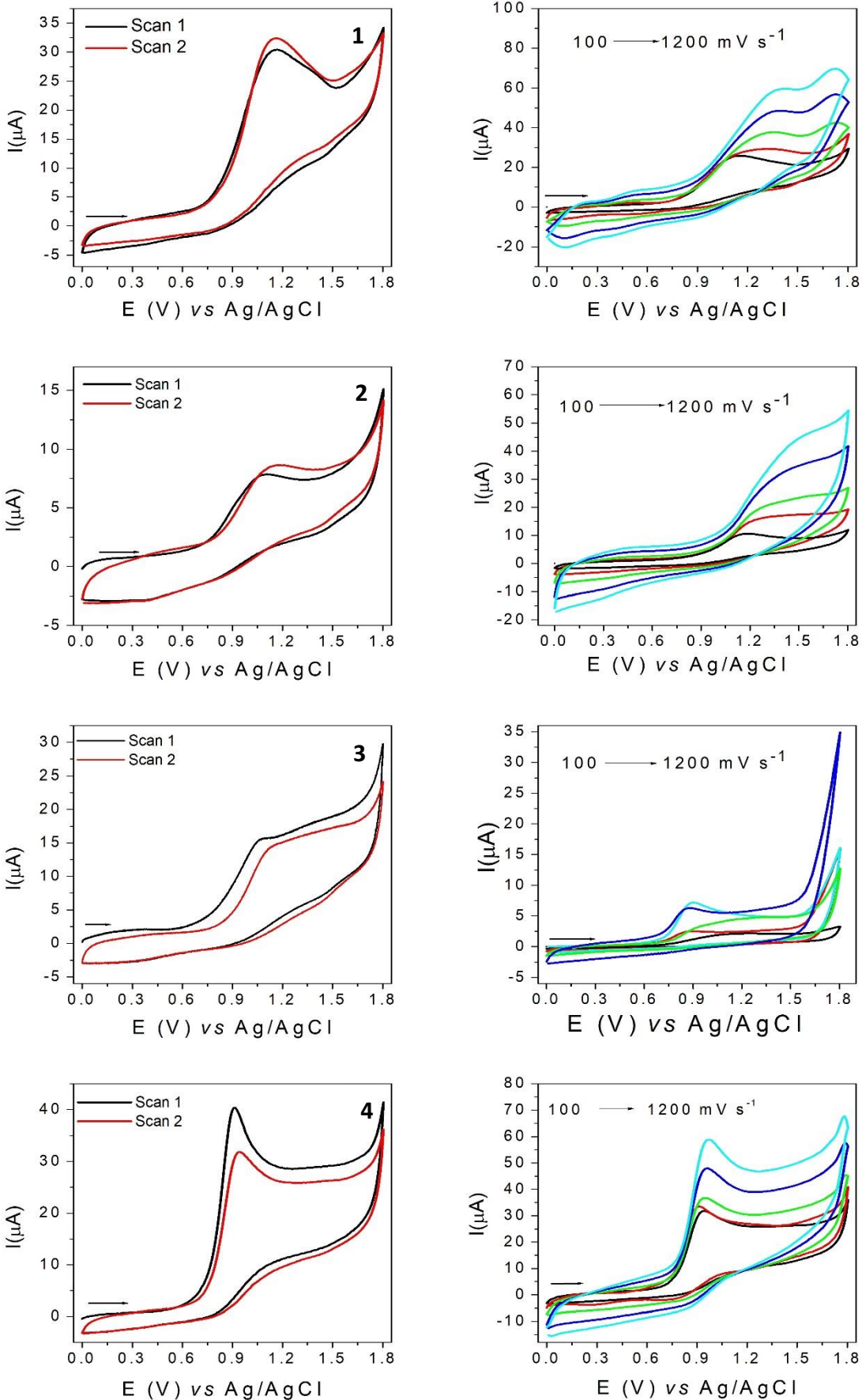


Figure S10. Cyclic voltammograms of phosphines **1** - **4** in $\text{CH}_3\text{CN}/[\text{nBu}_4\text{N}][\text{ClO}_4]$ solutions vs. Ag/AgCl , 100 mV s^{-1} , and respective scan rates ($100, 200, 400, 800, 1200 \text{ mV s}^{-1}$).

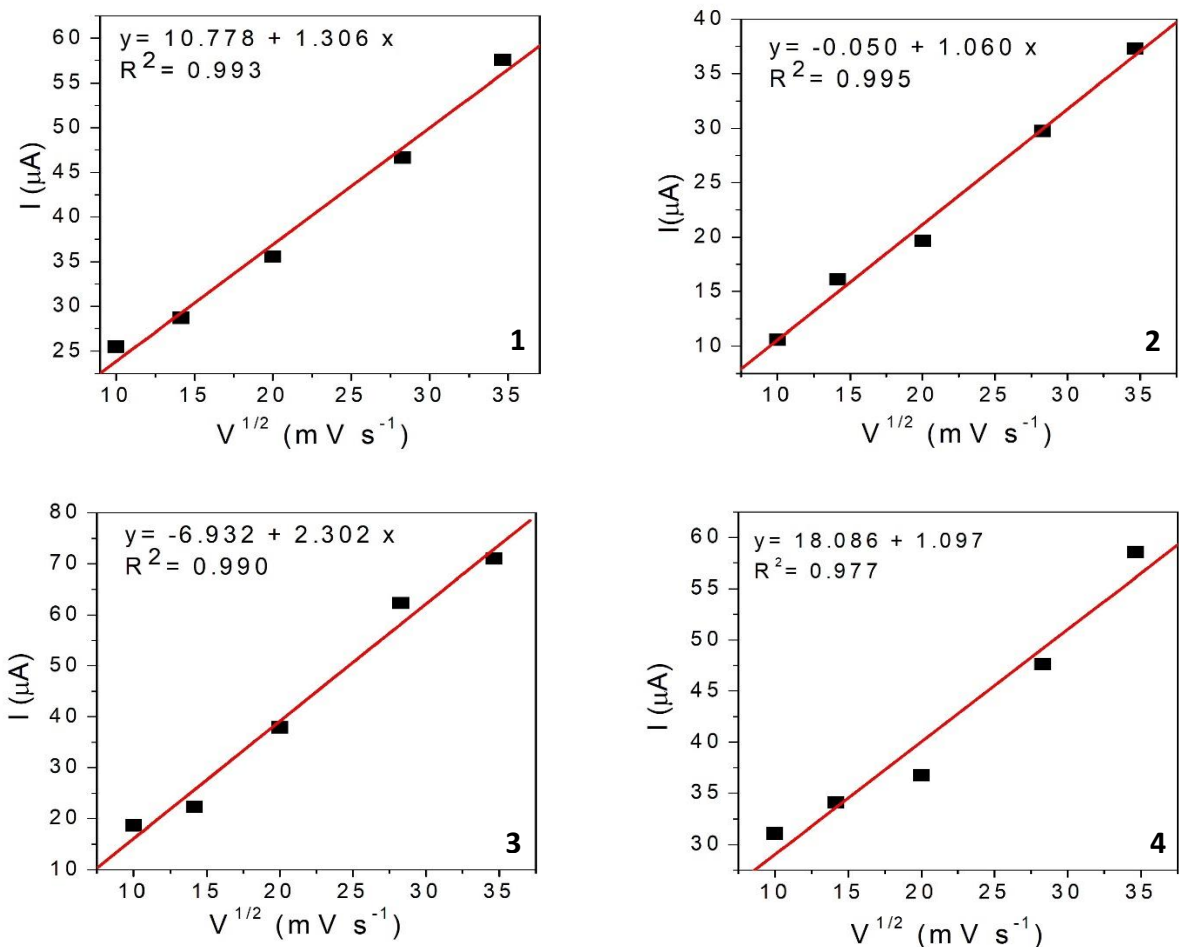


Figure S11. Dependence of the peak current variation for the phosphines **1** - **4** with root square of scanning rate ($100, 200, 400, 800, 1200 \text{ mV s}^{-1}$).

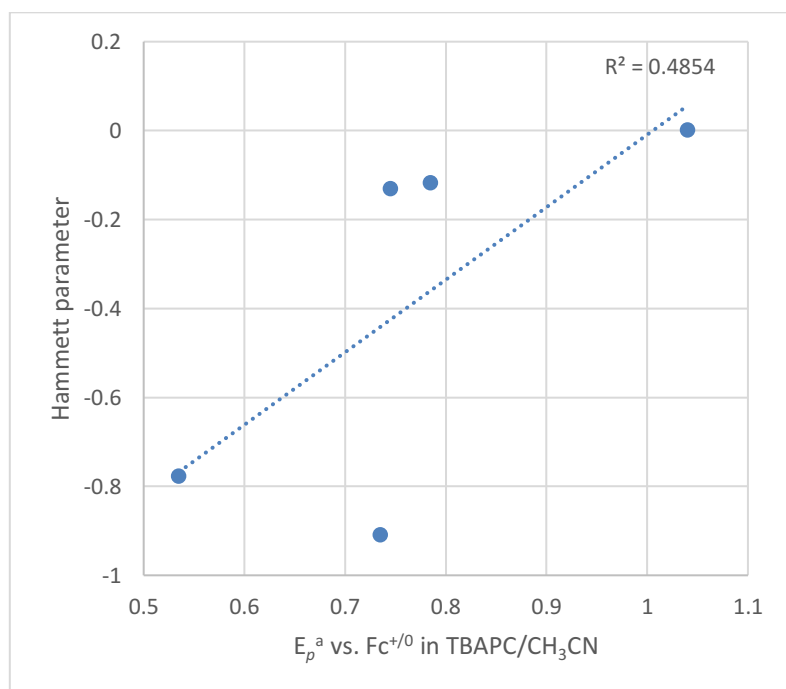


Figure S12. Correlation between E_p^a and estimated Hammett σ^+ parameters for multiple substituents.

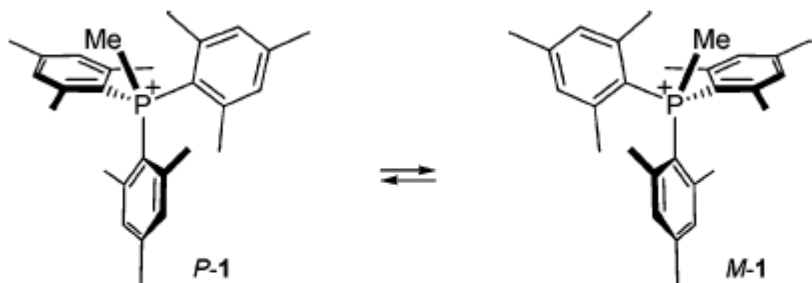
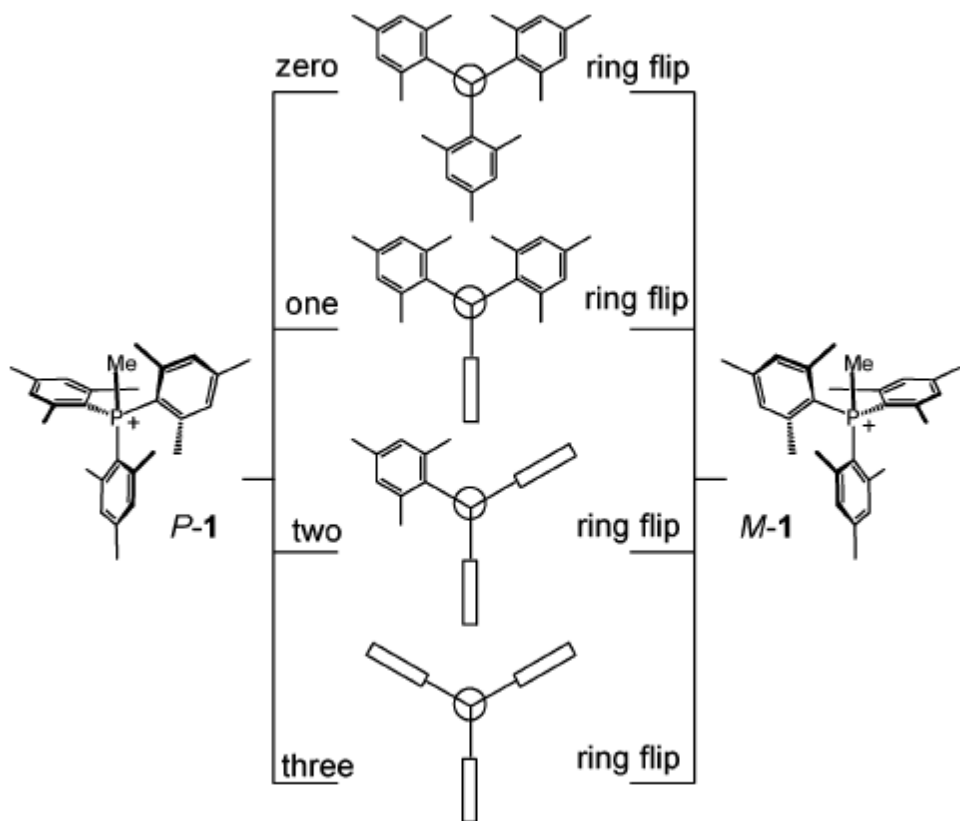


FIGURE 1. Interconverting helical configurations (*P* and *M*) of trimesitylmethylphosphonium cation **1**.
(a)

SCHEME 1. The Four Possible Flip Processes for the Enantiomerization of Cation **1**^a



^a Structures in the middle represent the four transition states viewed along the P^+-CH_3 bond.
(b)

Figure S13. (a) Perspective drawing of the *P* and *M* conformers for pyramidal propeller molecules. (b) Perspective views (viewed from above) of the classical 'flip' processes for racemization of such molecules. (Reprinted with permission from B. Laleu, G. Bernardinelli, R. Chauvin, J. Lacour, *J. Org. Chem.* **2006**, *71*, 7412-7416. Copyright 2006 American Chemical Society.)²

DFT Calculations

Gas-phase hybrid density functional theory (DFT) calculations at the B3LYP/6-31G(2d,p) level of theory were conducted using Gaussian W03 (or in part, GW16).^{3,4} Results were interpreted using GaussView6.⁵ Archival geometries from the DFT Structure optimizations are provided in the following tables. Dispersion-corrected geometries using Grimme's D3 empirical factors follow after the non-corrected geometries.

Phosphine **1** (gas phase singlet electronic state; B3LYP/6-31G(2d,p))

Tag	Symbol	NA	NB	NC	Bond	Angle	Dihedral	X	Y	Z
1	C							2.363276	1.009109	-0.089828
1	P							0	0	1.675994
2	C	1			2.778184			1.616659	-2.2496	1.466213
3	H	2	1		1.083899	81.8427		1.061164	-2.54129	2.350056
4	C	1	2	3	4.176694	130.3596	-177.163	-0.30164	3.353918	-0.79484
5	C	4	1	2	1.539224	137.3061	89.61666	-1.11761	3.780735	-2.02823
6	C	1	2	4	1.848891	99.89348	95.38967	-1.53749	-0.63752	0.870946
7	C	4	1	6	1.394589	99.86397	167.8868	0.635438	4.186241	-0.18329
8	H	7	4	1	1.082609	119.0179	-179.325	0.800335	5.177134	-0.587
9	C	2	1	6	2.806721	96.80835	99.27005	3.0554	-1.41573	-0.79484
10	C	2	1	6	1.393222	157.9094	99.04283	2.600549	-3.08841	0.947145
11	C	6	1	2	1.404159	116.6414	139.4501	-2.75654	-0.27527	1.466213
12	H	11	6	1	1.083899	118.3443	0.198154	-2.73141	0.351652	2.350056
13	C	4	1	6	1.403648	17.87666	-14.1548	-0.49327	2.074771	-0.2496
14	H	13	4	1	1.083672	119.7739	178.2151	-1.20754	1.397837	-0.70339
15	C	7	4	1	2.545497	154.4283	0.044545	2.387847	4.774809	1.566626
16	C	9	2	1	1.394588	58.52808	179.9132	3.307672	-2.64343	-0.18329
17	H	16	9	2	1.082609	119.0179	-179.383	4.083362	-3.28168	-0.587
18	C	9	2	1	1.403649	59.20339	-0.7563	2.043437	-0.6102	-0.2496
19	H	18	9	2	1.083673	119.7739	179.8425	1.81433	0.346839	-0.70339
20	C	18	9	2	1.392763	121.3792	-0.08072	1.32085	-1.01275	0.870946
21	C	13	4	1	1.392763	121.3793	-1.70813	0.216637	1.650262	0.870946
22	C	7	4	1	1.405673	122.7064	0.248303	1.374367	3.796346	0.947145
23	C	11	6	1	2.574825	151.5808	179.8342	-5.32903	-0.31947	1.566626
24	C	11	6	1	2.394887	90.09245	-178.978	-3.94311	-1.54282	-0.18329
25	H	24	11	6	1.082609	149.2836	179.5942	-4.8837	-1.89546	-0.587
26	C	24	11	6	1.394588	91.69281	0.65002	-2.75376	-1.93819	-0.79484
27	C	11	6	1	1.393223	121.41	-179.563	-3.97492	-0.70794	0.947145
28	C	10	2	1	1.538924	122.7596	179.8794	2.941183	-4.45534	1.566626
29	C	5	4	1	1.545952	109.3973	-60.3158	-0.83214	2.807209	-3.19473
30	H	29	5	4	1.095062	110.9107	-61.141	0.227628	2.826929	-3.46981
31	H	29	5	4	1.095843	110.3859	179.1937	-1.41662	3.088116	-4.0781
32	H	29	5	4	1.093446	111.8433	59.27606	-1.09216	1.77674	-2.93754
33	C	22	7	4	1.393222	117.6635	-0.36885	1.139884	2.524869	1.466213
34	H	33	22	7	1.083899	120.2454	-178.631	1.670242	2.189641	2.350056
35	C	5	4	1	1.538977	112.4929	179.5095	-0.77277	5.205034	-2.49824
36	H	35	5	4	1.094701	111.8887	-60.5131	-0.97672	5.951045	-1.72348
37	H	35	5	4	1.094823	109.7242	-179.703	-1.38068	5.463338	-3.37136
38	H	35	5	4	1.094746	111.8719	61.13158	0.278124	5.294431	-2.79168
39	C	5	4	1	1.546159	109.2569	59.32288	-2.62409	3.737508	-1.68292

40	H	39	5	4	1.093497	111.8304	-58.8778	-2.94065	2.739275	-1.36819
41	H	39	5	4	1.095779	110.3925	-178.923	-3.22403	4.020105	-2.55525
42	H	39	5	4	1.094806	110.8242	61.38251	-2.85732	4.433422	-0.87058
43	C	23	11	6	1.546054	120.5707	73.29782	-6.07664	-1.59647	2.014528
44	H	43	23	11	1.093609	111.9197	-86.978	-6.25932	-2.27711	1.178259
45	H	43	23	11	1.09576	110.3316	153.1247	-7.04776	-1.33607	2.450194
46	H	43	23	11	1.094693	110.9406	33.38814	-5.50131	-2.1423	2.769123
47	C	6	1	21	1.392763	124.239	94.22419	-1.55017	-1.46457	-0.2496
48	H	47	6	1	1.083673	118.8467	-1.35672	-0.60679	-1.74468	-0.70339
49	C	26	24	11	1.539224	122.8264	179.4785	-2.71541	-2.85824	-2.02823
50	C	9	2	1	2.51789	144.2824	-57.8977	2.847182	-0.68295	-3.19473
51	H	50	9	2	1.095062	91.81225	-57.323	2.334378	-1.6106	-3.46981
52	H	50	9	2	1.095844	145.5933	176.278	3.382695	-0.31723	-4.0781
53	H	50	9	2	1.093445	91.75028	50.58296	2.084782	0.057468	-2.93754
54	C	15	7	4	1.545915	93.72036	125.4234	3.462049	5.136175	0.515266
55	H	54	15	7	1.094773	110.9082	-84.9425	3.999982	4.242369	0.1832
56	H	54	15	7	1.095731	110.3583	155.3639	4.192498	5.833361	0.94071
57	H	54	15	7	1.093517	111.9181	35.46883	3.025458	5.610689	-0.36791
58	C	15	7	4	1.539053	140.9858	0.377054	3.101319	4.177496	2.792538
59	H	58	15	7	1.094517	111.9212	-61.2337	2.398317	3.9301	3.594131
60	H	58	15	7	1.094795	109.675	179.534	3.815701	4.903809	3.193416
61	H	58	15	7	1.094509	111.8081	60.28846	3.659478	3.271431	2.536695
62	C	9	2	1	1.539224	178.5754	17.83273	3.833015	-0.92249	-2.02823
63	C	15	7	4	1.546052	93.75455	-124.863	1.655736	6.060762	2.014528
64	H	63	15	7	1.093609	111.9197	-35.001	1.15763	6.559285	1.178259
65	H	63	15	7	1.09576	110.3316	-154.898	2.366813	6.771575	2.450194
66	H	63	15	7	1.094693	110.9407	85.3652	0.895367	5.835424	2.769123
67	C	62	9	2	1.538976	112.4929	162.1547	4.894074	-1.93328	-2.49824
68	H	67	62	9	1.094701	111.8888	-60.513	5.642117	-2.12966	-1.72348
69	H	67	62	9	1.094823	109.7242	-179.703	5.421731	-1.53596	-3.37136
70	H	67	62	9	1.094746	111.8719	61.13158	4.44605	-2.88808	-2.79168
71	C	23	11	6	1.539054	85.2169	-178.419	-5.16848	0.597074	2.792538
72	H	71	23	11	1.094518	111.9211	-60.9336	-4.60272	0.111954	3.594131
73	H	71	23	11	1.094795	109.675	179.8341	-6.15467	0.85259	3.193416
74	H	71	23	11	1.094508	111.8081	60.58858	-4.66288	1.533485	2.536695
75	C	23	11	6	1.545915	120.9657	-70.1825	-6.17908	0.430135	0.515266
76	H	75	23	11	1.094773	110.9082	-33.1413	-5.67399	1.342902	0.1832
77	H	75	23	11	1.095732	110.3583	-152.835	-7.14809	0.714129	0.94071
78	H	75	23	11	1.093518	111.9181	87.27012	-6.37173	-0.18522	-0.36791
79	C	62	9	2	1.54616	109.2569	41.96817	4.548824	0.403778	-1.68292
80	H	79	62	9	1.093498	111.8305	-58.8778	3.842605	1.177038	-1.36819
81	H	79	62	9	1.095778	110.3925	-178.923	5.093526	0.782036	-2.55525
82	H	79	62	9	1.094805	110.8242	61.38242	5.268114	0.2578	-0.87058
83	C	49	26	24	1.545951	109.3974	120.5266	-2.01505	-2.12426	-3.19473
84	H	83	49	26	1.095063	110.9106	-61.1409	-2.56201	-1.21633	-3.46981
85	H	83	49	26	1.095843	110.3859	179.1938	-1.96608	-2.77088	-4.0781
86	H	83	49	26	1.093445	111.8433	59.27603	-0.99262	-1.83421	-2.93754
87	C	49	26	24	1.538977	112.4929	0.351803	-4.12131	-3.27175	-2.49824
88	H	87	49	26	1.094701	111.8887	-60.5131	-4.6654	-3.82139	-1.72348

89	H	87	49	26	1.094823	109.7242	-179.703	-4.04105	-3.92738	-3.37136
90	H	87	49	26	1.094745	111.8719	61.13159	-4.72417	-2.40635	-2.79168
91	C	28	10	2	1.546052	109.4881	-119.546	4.420906	-4.46429	2.014528
92	H	91	28	10	1.093609	111.9197	-59.6059	5.101693	-4.28218	1.178259
93	H	91	28	10	1.09576	110.3316	-179.503	4.68095	-5.43551	2.450194
94	H	91	28	10	1.094692	110.9407	60.76032	4.605941	-3.69312	2.769123
95	C	28	10	2	1.545915	109.4189	120.602	2.717034	-5.56631	0.515266
96	H	95	28	10	1.094773	110.9082	-60.3193	1.674009	-5.58527	0.1832
97	H	95	28	10	1.095732	110.3583	179.9872	2.955591	-6.54749	0.94071
98	H	95	28	10	1.093518	111.9181	60.09215	3.346271	-5.42547	-0.36791
99	C	28	10	2	1.539054	112.2826	0.59938	2.067158	-4.77457	2.792538
100	H	99	28	10	1.094518	111.9211	-61.2073	2.204408	-4.04205	3.594131
101	H	99	28	10	1.094795	109.675	179.5604	2.338973	-5.7564	3.193416
102	H	99	28	10	1.094509	111.8081	60.31485	1.003404	-4.80492	2.536695
103	C	49	26	24	1.546159	109.2568	-119.835	-1.92473	-4.14129	-1.68292
104	H	103	49	26	1.093497	111.8305	-58.8778	-0.90196	-3.91631	-1.36819
105	H	103	49	26	1.09578	110.3925	-178.923	-1.8695	-4.80214	-2.55525
106	H	103	49	26	1.094806	110.8242	61.38253	-2.4108	-4.69122	-0.87058

Phosphine **2** (gas phase singlet electronic state; B3LYP/6-31G(2d,p))

Tag	Symbol	NA	NB	NC	Bond	Angle	Dihedral	X	Y	Z
1	P							-0.00285	-0.00109	-1.37934
2	C	1			1.848423			1.263941	-1.08625	-0.5829
3	C	2	1		1.400538	116.6638		2.50909	-1.16982	-1.21861
4	C	2	1	3	1.398766	124.5281	-178.318	1.046714	-1.84064	0.574792
5	C	3	2	1	1.396374	121.4048	-179.627	3.535356	-1.96649	-0.70679
6	C	5	3	2	1.397491	118.34	1.333884	3.284375	-2.70944	0.449941
7	C	6	5	3	1.396896	121.7352	-0.41784	2.048044	-2.66397	1.098583
8	C	5	3	2	1.509913	120.8091	-178.022	4.886946	-2.01229	-1.37831
9	H	6	5	3	1.087728	119.1324	179.112	4.069946	-3.34565	0.851518
10	C	7	6	5	1.510245	120.6932	178.2948	1.789751	-3.50593	2.325458
11	C	1	2	4	1.84832	102.6407	91.59387	0.307799	1.636625	-0.5808
12	C	11	1	2	1.400775	116.6579	164.6005	-0.26329	2.756012	-1.19967
13	C	12	11	1	1.396026	121.4112	-179.662	-0.08621	4.041483	-0.68479
14	C	13	12	11	1.397717	118.3466	1.342273	0.704377	4.195776	0.457476
15	C	14	13	12	1.396697	121.7192	-0.40835	1.304192	3.10357	1.088405
16	C	11	1	2	1.398397	124.539	-13.7304	1.091129	1.825566	0.5621
17	C	13	12	11	1.509888	120.8172	-178.013	-0.74449	5.23349	-1.33713
18	H	14	13	12	1.087722	119.1226	179.1104	0.862744	5.193442	0.860863
19	C	15	14	13	1.510182	120.7431	178.265	2.185864	3.299706	2.298709
20	C	1	11	16	1.848387	102.6327	92.55184	-1.57247	-0.55237	-0.57378
21	C	20	1	11	1.399296	116.6363	162.2137	-2.28531	-1.56901	-1.21902
22	C	20	1	11	1.400365	124.5601	-15.9791	-2.09953	0.000118	0.600099
23	C	21	20	1	1.397463	121.4115	-179.328	-3.49169	-2.05192	-0.70486
24	C	23	21	20	1.396195	118.3418	1.188805	-3.99094	-1.47686	0.465361
25	C	22	20	1	1.396981	121.0962	178.4212	-3.31098	-0.45134	1.129365
26	C	23	21	20	1.509929	120.789	-178.45	-4.23179	-3.17326	-1.39386
27	H	24	23	21	1.087955	119.1072	178.8345	-4.93872	-1.83014	0.866043

28	C	25	22	20	1.510513	120.9622	-179.922	-3.87758	0.147977	2.394841
29	H	21	20	1	1.087244	119.33	0.030337	-1.89808	-1.98541	-2.14571
30	H	22	20	1	1.085102	119.664	-1.1413	-1.56437	0.79711	1.105918
31	H	8	5	3	1.093827	111.3677	-29.1841	4.804244	-1.82849	-2.45341
32	H	10	7	6	1.093716	111.3813	154.1319	1.018833	-3.05979	2.960167
33	H	3	2	1	1.087253	119.3371	0.205691	2.68007	-0.60472	-2.13159
34	H	4	2	1	1.085074	119.6491	-1.25792	0.084718	-1.79221	1.074395
35	H	12	11	1	1.087303	119.3433	0.175416	-0.85514	2.622021	-2.10188
36	H	16	11	1	1.085225	119.7068	-1.22529	1.547147	0.969635	1.049074
37	H	26	23	21	1.094033	111.4607	-150.22	-5.3116	-3.0969	-1.23542
38	H	26	23	21	1.093834	111.3777	-29.3499	-4.04478	-3.17138	-2.47159
39	H	26	23	21	1.097131	111.2092	90.16371	-3.91536	-4.15163	-1.01129
40	H	28	25	22	1.095715	111.3307	123.7451	-4.8896	0.53587	2.23376
41	H	28	25	22	1.093042	111.3328	3.331466	-3.25662	0.971082	2.757679
42	H	28	25	22	1.096406	111.4052	-116.981	-3.94513	-0.59799	3.195509
43	H	17	13	12	1.093819	111.3653	-29.2945	-0.88061	5.075459	-2.41088
44	H	17	13	12	1.097134	111.2129	90.23113	-1.73644	5.423139	-0.90844
45	H	17	13	12	1.094085	111.4646	-150.16	-0.15243	6.14312	-1.19909
46	H	19	15	14	1.093906	111.399	151.233	2.164103	2.424383	2.954427
47	H	19	15	14	1.094154	111.4987	30.30752	1.876316	4.171256	2.883306
48	H	19	15	14	1.097138	111.1788	-89.2988	3.23112	3.459294	2.005991
49	H	10	7	6	1.09426	111.4905	33.22174	2.696482	-3.62863	2.925614
50	H	8	5	3	1.094051	111.4674	-150.043	5.372533	-2.98216	-1.23509
51	H	8	5	3	1.097156	111.2156	90.34639	5.55974	-1.24838	-0.969
52	H	10	7	6	1.097135	111.1916	-86.3346	1.443877	-4.51043	2.051491

Phosphine **3** (gas phase singlet electronic state; B3LYP/6-31G(2d,p))

Tag	Symbol	NA	NB	NC	Bond	Angle	Dihedral	X	Y	Z
1	P							0.003357	-0.00279	-1.54541
2	C	1			1.852561			1.640881	-0.33057	-0.7435
3	C	2	1		1.4017	116.9078		2.774727	0.194307	-1.37884
4	C	2	1	3	1.401153	124.6707	-179.355	1.818262	-1.06986	0.433456
5	C	3	2	1	1.398255	121.9271	-179.757	4.062489	0.005974	-0.86765
6	C	5	3	2	1.404042	117.9473	1.151454	4.200475	-0.75479	0.304332
7	C	4	2	1	1.398846	121.5667	179.1113	3.089224	-1.29315	0.973423
8	C	5	3	2	1.509586	121.1878	-178.58	5.269175	0.605516	-1.54832
9	C	7	4	2	1.509565	121.2448	178.9608	3.270119	-2.07105	2.254413
10	C	1	2	4	1.853398	102.699	89.86023	-0.53416	1.578832	-0.74253
11	C	10	1	2	1.402196	116.9594	164.9555	-1.58495	2.277209	-1.35431
12	C	11	10	1	1.397694	121.911	-179.47	-2.06519	3.486068	-0.84286
13	C	12	11	10	1.404521	117.9739	1.134384	-1.44588	4.00843	0.304434
14	C	13	12	11	1.403723	121.8374	-1.43453	-0.39566	3.336873	0.949783
15	C	14	13	12	1.399486	118.2681	0.886899	0.045722	2.123314	0.410319
16	C	12	11	10	1.509629	121.2371	-178.647	-3.21735	4.210077	-1.49656
17	C	14	13	12	1.509668	120.5595	-178.127	0.221278	3.903998	2.205513
18	C	1	2	4	1.853322	102.6665	-16.2869	-1.10067	-1.256	-0.74204
19	C	18	1	2	1.401638	117.0562	-90.696	-1.21583	-2.5021	-1.37335
20	C	18	1	2	1.401153	124.5314	89.96347	-1.82879	-1.03494	0.434485

21	C	19	18	1	1.398228	121.9211	-179.659	-2.02608	-3.51917	-0.85944
22	C	21	19	18	1.404266	117.9638	1.125091	-2.75405	-3.25284	0.311501
23	C	20	18	1	1.398923	121.5861	178.9989	-2.66116	-2.01972	0.977012
24	C	21	19	18	1.509636	121.1717	-178.645	-2.11419	-4.86545	-1.53676
25	C	23	20	18	1.509649	121.1972	179.1798	-3.42757	-1.77864	2.255108
26	H	19	18	1	1.087968	119.4138	0.599395	-0.65793	-2.69127	-2.28802
27	H	20	18	1	1.085996	119.6907	-0.9971	-1.75085	-0.0789	0.943701
28	H	8	5	3	1.093242	110.7993	21.84171	4.979691	1.451573	-2.17725
29	H	9	7	4	1.092983	110.7783	-10.1026	2.307272	-2.2456	2.741312
30	H	3	2	1	1.087951	119.403	0.533031	2.655591	0.769904	-2.29434
31	H	4	2	1	1.086029	119.7007	-0.9434	0.953724	-1.48209	0.945409
32	H	11	10	1	1.088005	119.4333	0.804277	-2.04724	1.869667	-2.25094
33	H	15	14	13	1.085946	118.6982	-179.811	0.855732	1.596327	0.905746
34	H	24	21	19	1.097268	111.7987	-97.0637	-2.99138	-4.93517	-2.19226
35	H	24	21	19	1.093307	110.8054	22.44546	-1.23215	-5.04668	-2.15682
36	H	24	21	19	1.09297	110.9165	143.3543	-2.19696	-5.66835	-0.79981
37	H	25	23	20	1.096779	111.7907	107.2838	-4.49966	-1.64305	2.06756
38	H	25	23	20	1.092996	110.7621	-12.4393	-3.06754	-0.87788	2.758741
39	H	25	23	20	1.093597	111.1007	-133.474	-3.33046	-2.62696	2.938394
40	H	16	12	11	1.093235	110.7952	21.1746	-3.80921	3.524604	-2.10892
41	H	16	12	11	1.093006	110.9288	142.1134	-3.86943	4.664112	-0.74602
42	H	16	12	11	1.097247	111.8054	-98.3824	-2.87103	5.017143	-2.15433
43	H	17	14	13	1.093029	110.7682	166.4211	0.844097	3.156246	2.703183
44	H	17	14	13	1.093626	111.063	45.43712	-0.54937	4.241495	2.904232
45	H	17	14	13	1.096758	111.851	-73.8375	0.858198	4.770917	1.991827
46	H	9	7	4	1.093828	111.0801	-131.064	3.923903	-1.53703	2.950003
47	H	8	5	3	1.097221	111.8066	-97.6853	5.775406	-0.12174	-2.1954
48	H	8	5	3	1.093007	110.9162	142.7664	6.001884	0.947984	-0.81312
49	H	9	7	4	1.096501	111.8418	109.742	3.730471	-3.05005	2.075637
50	O	13	12	11	1.387031	119.2656	-178.085	-1.92672	5.185799	0.858019
51	O	6	5	3	1.386991	119.4287	-177.961	5.458981	-0.92543	0.861817
52	O	22	21	19	1.386931	119.4345	-178.064	-3.53591	-4.25285	0.870274
53	C	52	22	21	1.426359	114.835	-88.6741	-4.87225	-4.31537	0.375491
54	H	53	52	22	1.097164	111.7107	63.08327	-4.89775	-4.54979	-0.69604
55	H	53	52	22	1.092206	106.6009	-177.856	-5.37236	-5.11413	0.927576
56	H	53	52	22	1.097219	111.6228	-58.7437	-5.40904	-3.37279	0.540626
57	C	50	13	12	1.426287	114.7768	-89.7123	-1.32954	6.3751	0.344954
58	H	57	50	13	1.097223	111.6966	62.54037	-1.52517	6.497015	-0.72778
59	H	57	50	13	1.092219	106.6048	-178.373	-1.77963	7.209432	0.887401
60	H	57	50	13	1.097219	111.6358	-59.272	-0.24426	6.384848	0.506123
61	C	51	6	5	1.426455	114.873	-88.7976	6.185188	-2.05069	0.37071
62	H	61	51	6	1.097129	111.7506	62.79907	6.395303	-1.96209	-0.70246
63	H	61	51	6	1.0922	106.5838	-178.142	7.129872	-2.07519	0.918316
64	H	61	51	6	1.097244	111.6289	-59.0489	5.643693	-2.98894	0.545076

Phosphine **4** (gas phase singlet electronic state; B3LYP/6-31G(2d,p))

Tag	Symbol	NA	NB	NC	Bond	Angle	Dihedral	X	Y	Z
1	P							0.003357	-0.00279	-1.54541
1	P							-0.0924	0.020196	1.511134
2	C	1			1.850754			0.693346	1.466027	0.664099
3	C	2	1		1.401084	117.3916		1.732356	2.12129	1.337987
4	C	2	1	3	1.406743	124.9164	-178.538	0.306197	1.972457	-0.58992
5	C	3	2	1	1.396492	121.8812	-179.726	2.386907	3.225694	0.7884
6	C	5	3	2	1.399741	119.4194	0.873797	1.987554	3.708992	-0.46309
7	C	4	2	1	1.389057	121.2185	179.0998	0.939112	3.076245	-1.14719
8	C	1	2	3	1.850782	102.7749	-94.3309	0.845546	-1.41805	0.820416
9	C	8	1	2	1.408687	117.3226	164.7921	0.72658	-2.6504	1.4924
10	C	9	8	1	1.387305	121.491	-179.339	1.402463	-3.78118	1.057488
11	C	10	9	8	1.403204	120.0141	0.897709	2.242124	-3.70892	-0.06444
12	C	11	10	9	1.398884	119.5324	-0.11511	2.388772	-2.49208	-0.73872
13	C	12	11	10	1.3984	119.6913	-0.42013	1.691217	-1.3649	-0.29329
14	C	1	2	3	1.850904	102.6669	159.5358	-1.72501	-0.11664	0.649908
15	C	14	1	2	1.401016	117.3738	-93.4726	-2.8168	0.541923	1.23053
16	C	14	1	2	1.40685	124.9376	87.86405	-1.95613	-0.85271	-0.52653
17	C	15	14	1	1.396307	121.8803	-179.914	-4.09117	0.499834	0.661413
18	C	17	15	14	1.399812	119.4363	0.871522	-4.29622	-0.23373	-0.51303
19	C	16	14	1	1.389188	121.2098	179.3209	-3.21948	-0.9136	-1.10106
20	H	15	14	1	1.087183	119.4364	-0.11807	-2.67516	1.100747	2.152279
21	H	16	14	1	1.085605	119.7308	-0.2159	-1.13767	-1.39108	-0.99431
22	H	3	2	1	1.087162	119.4134	0.024743	2.039634	1.766992	2.31879
23	H	4	2	1	1.085427	119.7135	-0.43624	-0.50639	1.500511	-1.13318
24	H	9	8	1	1.087148	119.5113	0.447868	0.094614	-2.72072	2.374197
25	H	13	12	11	1.085477	118.5633	179.8166	1.820871	-0.42936	-0.82828
26	O	11	10	9	1.365007	115.7154	179.5457	2.870875	-4.87034	-0.40944
27	O	6	5	3	1.364869	124.7055	179.4802	2.543431	4.783739	-1.09458
28	O	18	17	15	1.364816	124.6852	179.5495	-5.49519	-0.35486	-1.15375
29	C	28	18	17	1.419019	118.2147	0.186893	-6.62114	0.308984	-0.60133
30	H	29	28	18	1.097474	111.6616	60.91929	-6.47219	1.395625	-0.56294
31	H	29	28	18	1.090913	106.0341	179.7527	-7.45819	0.084851	-1.26406
32	H	29	28	18	1.097451	111.6661	-61.4262	-6.8521	-0.05614	0.407501
33	C	26	11	10	1.418883	118.2095	-179.524	3.74087	-4.8547	-1.5302
34	H	33	26	11	1.097503	111.6756	61.04323	4.577139	-4.15904	-1.38453
35	H	33	26	11	1.090944	106.0328	179.8792	4.130514	-5.86943	-1.62335
36	H	33	26	11	1.097522	111.6895	-61.2979	3.209621	-4.58646	-2.45236
37	C	27	6	5	1.418985	118.2422	-0.05391	3.602558	5.469891	-0.44576
38	H	37	27	6	1.097495	111.7024	61.19965	4.467452	4.815454	-0.27794
39	H	37	27	6	1.090938	106.0243	-179.989	3.891566	6.280528	-1.1162
40	H	37	27	6	1.097452	111.6799	-61.1768	3.282907	5.893286	0.514946
41	H	7	4	2	1.085331	121.3105	-179.747	0.638945	3.470677	-2.11273
42	H	5	3	2	1.083594	119.4416	-179.828	3.187445	3.700744	1.343056
43	H	12	11	10	1.083757	121.0415	179.6112	3.035662	-2.4071	-1.60408
44	H	10	9	8	1.085151	121.4121	-179.804	1.307432	-4.73062	1.574282
45	H	19	16	14	1.085327	121.2925	-179.792	-3.4	-1.48376	-2.00675
46	H	17	15	14	1.083539	119.4405	-179.805	-4.90689	1.026459	1.142367

Phosphine **1** (gas phase singlet electronic state; B3LYP-D3/6-31G(2d,p) with Grimme correction)

Tag	Symbol	NA	NB	NC	Bond	Angle	Dihedral	X	Y	Z
1	C							-0.001024	-0.000448	2.044668
1	P							1.185126	-2.49272	1.611847
2	C	1			2.778184			0.617977	-2.761075	2.495327
3	H	2	1		1.083899	81.8427		0.19335	3.143698	-0.674603
4	C	1	2	3	4.176694	130.3596	-177.163	-0.584502	3.562351	-1.930889
5	C	4	1	2	1.539224	137.3061	89.61666	-1.57911	-0.407864	1.168577
6	C	1	2	4	1.848891	99.89348	95.38967	1.336251	3.799505	-0.222242
7	C	4	1	6	1.394589	99.86397	167.8868	1.700648	4.662273	-0.764543
8	H	7	4	1	1.082609	119.0179	-179.325	2.624283	-1.73744	-0.677157
9	C	2	1	6	2.806721	96.80835	99.27005	1.908797	-3.460031	0.917076
10	C	2	1	6	1.393222	157.9094	99.04283	-2.752326	0.219988	1.61244
11	C	6	1	2	1.404159	116.6414	139.4501	-2.700575	0.845367	2.49586
12	H	11	6	1	1.083899	118.3443	0.198154	-0.24034	2.019617	0.0398
13	C	4	1	6	1.403648	17.87666	-14.1548	-1.104683	1.47155	-0.309817
14	H	13	4	1	1.083672	119.7739	178.2151	3.316204	4.136588	1.333931
15	C	7	4	1	2.545497	154.4283	0.044545	2.62442	-3.054818	-0.223834
16	C	9	2	1	1.394588	58.52808	179.9132	3.190848	-3.800806	-0.765963
17	H	16	9	2	1.082609	119.0179	-179.383	1.865847	-0.801253	0.037216
18	C	9	2	1	1.403649	59.20339	-0.7563	1.820165	0.220972	-0.313034
19	H	18	9	2	1.083673	119.7739	179.8425	1.141458	-1.162704	1.168296
20	C	18	9	2	1.392763	121.3792	-0.08072	0.43531	1.570515	1.169653
21	C	13	4	1	1.392763	121.3793	-1.70813	2.044917	3.380366	0.917996
22	C	7	4	1	1.405673	122.7064	0.248303	-5.2438	0.797868	1.334831
23	C	11	6	1	2.574825	151.5808	179.8342	-3.959732	-0.744627	-0.223055
24	C	11	6	1	2.394887	90.09245	-178.978	-4.889119	-0.86134	-0.765149
25	H	24	11	6	1.082609	149.2836	179.5942	-2.81931	-1.403972	-0.676557
26	C	24	11	6	1.394588	91.69281	0.65002	-3.95215	0.077521	0.918012
27	C	11	6	1	1.393223	121.41	-179.563	1.931756	-4.938887	1.333524
28	C	10	2	1	1.538924	122.7596	179.8794	-0.517257	2.414797	-2.965385
29	C	5	4	1	1.545952	109.3973	-60.3158	0.519772	2.210045	-3.251415
30	H	29	5	4	1.095062	110.9107	-61.141	-1.073773	2.681742	-3.870875
31	H	29	5	4	1.095843	110.3859	179.1937	-0.943467	1.488346	-2.570414
32	H	29	5	4	1.093446	111.8433	59.27606	1.567204	2.27071	1.612603
33	C	22	7	4	1.393222	117.6635	-0.36885	2.083321	1.912133	2.495343
34	H	33	22	7	1.083899	120.2454	-178.631	-0.013166	4.834815	-2.57775
35	C	5	4	1	1.538977	112.4929	179.5095	-0.041597	5.685467	-1.889093
36	H	35	5	4	1.094701	111.8887	-60.5131	-0.604687	5.100761	-3.459536
37	H	35	5	4	1.094823	109.7242	-179.703	1.021646	4.693112	-2.905812
38	H	35	5	4	1.094746	111.8719	61.13158	-2.060914	3.826029	-1.555702
39	C	5	4	1	1.546159	109.2569	59.32288	-2.539324	2.93654	-1.13578
40	H	39	5	4	1.093497	111.8304	-58.8778	-2.631412	4.124174	-2.442276
41	H	39	5	4	1.095779	110.3925	-178.923	-2.135981	4.628768	-0.81514
42	H	39	5	4	1.094806	110.8242	61.38251	-6.355645	-0.241865	1.597696
43	C	23	11	6	1.546054	120.5707	73.29782	-6.570421	-0.843081	0.709912
44	H	43	23	11	1.093609	111.9197	-86.978	-7.284125	0.259207	1.893037
45	H	43	23	11	1.09576	110.3316	153.1247	-6.065229	-0.924851	2.402304
46	H	43	23	11	1.094693	110.9406	33.38814	-1.629114	-1.216105	0.037662

47	C	6	1	21	1.392763	124.239	94.22419	-0.721575	-1.688675	-0.312657
48	H	47	6	1	1.083673	118.8467	-1.35672	-2.791854	-2.285539	-1.933759
49	C	26	24	11	1.539224	122.8264	179.4785	2.343093	-0.764589	-2.970035
50	C	9	2	1	2.51789	144.2824	-57.8977	1.651379	-1.564602	-3.254089
51	H	50	9	2	1.095062	91.81225	-57.323	2.850475	-0.415453	-3.876437
52	H	50	9	2	1.095844	145.5933	176.278	1.749583	0.06548	-2.576697
53	H	50	9	2	1.093445	91.75028	50.58296	4.353176	4.040712	0.191596
54	C	15	7	4	1.545915	93.72036	125.4234	4.612451	2.995896	-0.009467
55	H	54	15	7	1.094773	110.9082	-84.9425	5.271163	4.574192	0.462374
56	H	54	15	7	1.095731	110.3583	155.3639	3.975308	4.476144	-0.737687
57	H	54	15	7	1.093517	111.9181	35.46883	3.952182	3.555085	2.608229
58	C	15	7	4	1.539053	140.9858	0.377054	3.268951	3.60634	3.461792
59	H	58	15	7	1.094517	111.9212	-61.2337	4.849366	4.12656	2.866529
60	H	58	15	7	1.094795	109.675	179.534	4.252877	2.511672	2.471232
61	H	58	15	7	1.094509	111.8081	60.28846	3.373405	-1.272292	-1.93452
62	C	9	2	1	1.539224	178.5754	17.83273	2.974087	5.619564	1.598655
63	C	15	7	4	1.546052	93.75455	-124.863	2.560807	6.107744	0.711744
64	H	63	15	7	1.093609	111.9197	-35.001	3.873316	6.171499	1.893816
65	H	63	15	7	1.09576	110.3316	-154.898	2.238209	5.709752	2.403982
66	H	63	15	7	1.094693	110.9407	85.3652	4.195476	-2.400698	-2.578681
67	C	62	9	2	1.538976	112.4929	162.1547	4.947905	-2.796327	-1.888753
68	H	67	62	9	1.094701	111.8888	-60.513	4.720162	-2.020684	-3.460991
69	H	67	62	9	1.094823	109.7242	-179.703	3.559551	-3.229801	-2.905367
70	H	67	62	9	1.094746	111.8719	61.13158	-5.059586	1.637778	2.610377
71	C	23	11	6	1.539054	85.2169	-178.419	-4.761375	1.019681	3.463032
72	H	71	23	11	1.094518	111.9211	-60.9336	-6.003872	2.127146	2.869371
73	H	71	23	11	1.094795	109.675	179.8341	-4.307541	2.421263	2.47448
74	H	71	23	11	1.094508	111.8081	60.58858	-5.680416	1.745007	0.193898
75	C	23	11	6	1.545915	120.9657	-70.1825	-4.905983	2.492989	-0.006308
76	H	75	23	11	1.094773	110.9082	-33.1413	-6.601867	2.271995	0.465637
77	H	75	23	11	1.095732	110.3583	-152.835	-5.868306	1.201163	-0.736086
78	H	75	23	11	1.093518	111.9181	87.27012	4.334082	-0.119646	-1.562334
79	C	62	9	2	1.54616	109.2569	41.96817	3.798666	0.737761	-1.144572
80	H	79	62	9	1.093498	111.8305	-58.8778	5.068597	-0.450342	-0.820988
81	H	79	62	9	1.095778	110.3925	-178.923	-1.834376	-1.649821	-2.968469
82	H	79	62	9	1.094805	110.8242	61.38242	-	-	-
83	C	49	26	24	1.545951	109.3974	120.5266	-2.178113	-0.649657	-3.252546
84	H	83	49	26	1.095063	110.9106	-61.1409	-1.787009	-2.263782	-3.874947
85	H	83	49	26	1.095843	110.3859	179.1938	-0.818702	-1.554049	-2.574519
86	H	83	49	26	1.093445	111.8433	59.27603	-4.17981	-2.429993	-2.579317
87	C	49	26	24	1.538977	112.4929	0.351803	-4.900303	-2.882654	-1.890364
88	H	87	49	26	1.094701	111.8887	-60.5131	-4.113575	-3.074035	-3.461924
89	H	87	49	26	1.094823	109.7242	-179.703	-4.577498	-1.463678	-2.905855
90	H	87	49	26	1.094745	111.8719	61.13159	3.388483	-5.380837	1.596166
91	C	28	10	2	1.546052	109.4881	-119.546	4.016377	-5.265264	0.708391
92	H	91	28	10	1.093609	111.9197	-59.6059	3.419683	-6.435572	1.890996
93	H	91	28	10	1.09576	110.3316	-179.503	3.834293	-4.787818	2.401014
94	H	91	28	10	1.094692	110.9407	60.76032	1.330372	-5.790762	0.192428
95	C	28	10	2	1.545915	109.4189	120.602	0.295084	-5.494939	-0.007531

96	H	95	28	10	1.094773	110.9082	-60.3193	1.335695	-6.852337	0.463842
97	H	95	28	10	1.095732	110.3583	179.9872	1.89502	-5.680788	-0.737636
98	H	95	28	10	1.093518	111.9181	60.09215	1.112575	-5.200196	2.609108
99	C	28	10	2	1.539054	112.2826	0.59938	1.498486	-4.63289	3.46189
100	H	99	28	10	1.094518	111.9211	-61.2073	1.161672	-6.2627	2.867801
101	H	99	28	10	1.094795	109.675	179.5604	0.057848	-4.941297	2.473417
102	H	99	28	10	1.094509	111.8081	60.31485	-2.277811	-3.695018	-1.560597
103	C	49	26	24	1.546159	109.2568	-119.835	-1.268046	-3.662313	-1.141417
104	H	103	49	26	1.093497	111.8305	-58.8778	-2.249655	-4.337046	-2.447938
105	H	103	49	26	1.09578	110.3925	-178.923	-2.933596	-4.164069	-0.820057
106	H	103	49	26	1.094806	110.8242	61.38253	-0.001024	-0.000448	2.044668

Phosphine **2** (gas phase singlet electronic state; B3LYP-D3/6-31G(2d,p) with Grimme correction)

Tag	Symbol	NA	NB	NC	Bond	Angle	Dihedral	X	Y	Z
1	P							0.000259	-0.00011	-1.46237
2	C	1			1.846572			-0.95929	-1.34524	-0.63791
3	C	2	1		1.400729	116.9568		-0.89265	-2.61912	-1.21654
4	C	2	1	3	1.397638	124.1054	179.7312	-1.72982	-1.16526	0.514172
5	C	3	2	1	1.395235	121.2755	178.686	-1.56036	-3.70668	-0.65257
6	C	5	3	2	1.398252	118.4213	1.189436	-2.32527	-3.49398	0.498419
7	C	6	5	3	1.395899	121.6722	-0.36048	-2.4255	-2.23324	1.089201
8	C	5	3	2	1.509556	120.9683	-177.962	-1.44692	-5.08574	-1.25597
9	H	6	5	3	1.087713	119.1225	179.2736	-2.86021	-4.33141	0.940759
10	C	7	6	5	1.50978	120.8314	178.3537	-3.28633	-2.01728	2.310578
11	C	1	2	4	1.846411	101.6067	91.50445	1.644906	-0.15816	-0.63812
12	C	11	1	2	1.400697	116.9667	167.1739	2.714905	0.535935	-1.21716
13	C	12	11	1	1.395278	121.2755	178.7016	3.990724	0.501302	-0.65335
14	C	13	12	11	1.398194	118.4251	1.192296	4.189002	-0.26708	0.497835
15	C	14	13	12	1.395941	121.6733	-0.36887	3.147176	-0.98369	1.089214
16	C	11	1	2	1.397796	124.1006	-13.0877	1.874351	-0.91496	0.514459
17	C	13	12	11	1.509552	120.9691	-177.969	5.1285	1.288358	-1.2573
18	H	14	13	12	1.087716	119.1244	179.2686	5.181794	-0.31181	0.939977
19	C	15	14	13	1.509785	120.8219	178.3399	3.390928	-1.83697	2.310666
20	C	1	11	16	1.846541	101.6103	91.48741	-0.6854	1.503455	-0.63844
21	C	20	1	11	1.400749	116.9512	167.3351	-1.82372	2.08045	-1.21585
22	C	20	1	11	1.397715	124.1114	-12.9154	-0.14289	2.083128	0.511895
23	C	21	20	1	1.395179	121.2769	178.6953	-2.43219	3.202392	-0.65235
24	C	23	21	20	1.398264	118.4219	1.202566	-1.86411	3.760937	0.496758
25	C	22	20	1	1.395871	121.6751	-0.36601	-0.72036	3.219832	1.086238
26	C	23	21	20	1.509542	120.9757	-177.971	-3.6849	3.791487	-1.25435
27	H	24	23	21	1.087731	119.1221	179.258	-2.32214	4.643085	0.938556
28	C	25	22	20	1.509771	120.8279	178.3414	-0.10144	3.860264	2.305333
29	H	21	20	1	1.087257	119.4391	-1.07436	-2.24445	1.644337	-2.11858
30	H	22	20	1	1.085048	119.751	0.236313	0.738516	1.646858	0.970285
31	H	8	5	3	1.093615	111.4481	-21.7861	-1.14669	-5.03911	-2.30654
32	H	10	7	6	1.09408	111.3514	150.588	-2.89509	-1.20921	2.935851
33	H	3	2	1	1.087262	119.4404	-1.09141	-0.30673	-2.76542	-2.12066
34	H	4	2	1	1.085072	119.7618	0.255769	-1.79062	-0.18417	0.973669

35	H	12	11	1	1.087254	119.4446	-1.08065	2.548779	1.116163	-2.12152
36	H	16	11	1	1.08505	119.7554	0.254041	1.055025	-1.4578	0.974207
37	H	26	23	21	1.0946	111.4278	-142.407	-3.67847	4.88475	-1.20065
38	H	26	23	21	1.093605	111.45	-21.5147	-3.79858	3.502885	-2.30304
39	H	26	23	21	1.096948	111.0429	98.20682	-4.5786	3.44635	-0.72004
40	H	28	25	22	1.097006	111.0155	-89.8424	0.644744	4.611687	2.018971
41	H	28	25	22	1.094067	111.3584	150.7812	0.407842	3.119764	2.929256
42	H	28	25	22	1.094188	111.5397	29.78759	-0.85328	4.365388	2.919191
43	H	17	13	12	1.09362	111.4516	-21.8413	4.938433	1.523786	-2.30823
44	H	17	13	12	1.096958	111.0401	97.86851	5.273957	2.238729	-0.72914
45	H	17	13	12	1.094578	111.4309	-142.74	6.072345	0.737353	-1.19688
46	H	19	15	14	1.09407	111.3614	150.8399	2.494603	-1.90544	2.934286
47	H	19	15	14	1.094189	111.5409	29.8401	4.204348	-1.43758	2.923927
48	H	19	15	14	1.097006	111.0091	-89.784	3.667891	-2.85983	2.026982
49	H	10	7	6	1.094181	111.543	29.59669	-3.35031	-2.92232	2.922169
50	H	8	5	3	1.094592	111.4321	-142.684	-2.39612	-5.62761	-1.19659
51	H	8	5	3	1.096954	111.0404	97.9248	-0.6973	-5.68677	-0.72669
52	H	10	7	6	1.097002	111.0147	-90.0409	-4.3096	-1.74179	2.026948

Phosphine **3** (gas phase singlet electronic state; B3LYP-D3/6-31G(2d,p) with Grimme correction)

Tag	Symbol	NA	NB	NC	Bond	Angle	Dihedral	X	Y	Z
1	P							0.000068	-0.00026	-1.64636
2	C	1			1.845486			-1.38873	-0.89389	-0.82266
3	C	2	1		1.400228	117.2033		-1.8072	-2.09851	-1.40096
4	C	2	1	3	1.397638	124.1772	179.0526	-2.02571	-0.45308	0.340665
5	C	3	2	1	1.394096	121.6608	178.7147	-2.82995	-2.86262	-0.84095
6	C	5	3	2	1.401583	118.122	0.956224	-3.45366	-2.38303	0.318966
7	C	4	2	1	1.397042	121.4773	-179.238	-3.06277	-1.18355	0.926024
8	C	5	3	2	1.507624	121.693	-178.896	-3.26452	-4.17185	-1.44925
9	C	7	4	2	1.508018	121.1113	179.4986	-3.73683	-0.70586	2.187597
10	C	1	2	4	1.845509	101.6026	90.49916	1.46831	-0.7559	-0.82224
11	C	10	1	2	1.400129	117.2052	166.7997	2.720615	-0.51741	-1.40122
12	C	11	10	1	1.394197	121.6668	178.7039	3.893842	-1.02079	-0.84092
13	C	12	11	10	1.401551	118.1149	0.953551	3.790335	-1.79897	0.320145
14	C	13	12	11	1.400084	121.8535	-0.96087	2.556097	-2.05878	0.92792
15	C	14	13	12	1.396946	118.2719	0.400238	1.405039	-1.52628	0.342285
16	C	12	11	10	1.507655	121.667	-178.926	5.244488	-0.74409	-1.45102
17	C	14	13	12	1.508001	120.5928	-178.919	2.480076	-2.8798	2.190538
18	C	1	2	4	1.84548	101.6028	-14.0789	-0.07966	1.649322	-0.82275
19	C	18	1	2	1.400196	117.2082	-88.6505	-0.91178	2.614769	-1.40245
20	C	18	1	2	1.397658	124.171	90.38516	0.61852	1.979731	0.342074
21	C	19	18	1	1.394125	121.6607	178.7025	-1.0623	3.882568	-0.84243
22	C	21	19	18	1.401575	118.1205	0.952201	-0.3372	4.182047	0.319011
23	C	20	18	1	1.397014	121.477	-179.224	0.504241	3.243004	0.927505
24	C	21	19	18	1.507632	121.6889	-178.908	-1.97671	4.914371	-1.45251
25	C	23	20	18	1.508015	121.1167	179.5067	1.252782	3.587209	2.190564
26	H	19	18	1	1.087277	119.4819	-0.83709	-1.46242	2.372434	-2.30812
27	H	20	18	1	1.085116	119.7584	0.103578	1.257522	1.241054	0.814842

28	H	8	5	3	1.092988	110.9746	15.01936	-2.52568	-4.53315	-2.1691
29	H	9	7	4	1.093305	110.8863	-24.6429	-3.0729	-0.05365	2.7613
30	H	3	2	1	1.087276	119.482	-0.82481	-1.32069	-2.45527	-2.3055
31	H	4	2	1	1.08512	119.7618	0.09294	-1.70687	0.470682	0.812353
32	H	11	10	1	1.087285	119.4827	-0.82582	2.786354	0.081125	-2.30655
33	H	15	14	13	1.085108	118.7664	-179.143	0.445655	-1.71086	0.814485
34	H	24	21	19	1.096643	111.5437	-104.665	-1.41145	5.690062	-1.983
35	H	24	21	19	1.092992	110.975	15.22714	-2.6603	4.455272	-2.17123
36	H	24	21	19	1.093184	110.8406	136.4558	-2.56106	5.421432	-0.68019
37	H	25	23	20	1.097001	111.457	94.83087	2.204343	4.086374	1.96971
38	H	25	23	20	1.093299	110.8875	-24.5245	1.485791	2.685708	2.763543
39	H	25	23	20	1.092684	110.8613	-145.777	0.668426	4.265968	2.816481
40	H	16	12	11	1.093007	110.9728	16.00338	5.191014	0.086534	-2.15944
41	H	16	12	11	1.093124	110.8383	137.2416	5.97895	-0.50494	-0.67752
42	H	16	12	11	1.096693	111.5363	-103.852	5.62747	-1.61671	-1.99378
43	H	17	14	13	1.093281	110.8917	155.1977	1.578831	-2.63699	2.759802
44	H	17	14	13	1.092698	110.8637	33.93126	3.356405	-2.70754	2.820109
45	H	17	14	13	1.096997	111.4558	-85.433	2.444944	-3.9537	1.969362
46	H	9	7	4	1.09268	110.8602	-145.892	-4.03441	-1.55059	2.813561
47	H	8	5	3	1.09663	111.5455	-104.882	-4.22021	-4.07277	-1.97786
48	H	8	5	3	1.093202	110.8428	136.2449	-3.40826	-4.93126	-0.67612
49	H	9	7	4	1.097001	111.4568	94.70898	-4.64387	-0.13049	1.964774
50	O	13	12	11	1.383183	118.6489	-178.068	4.950206	-2.27017	0.908242
51	O	6	5	3	1.38317	118.5876	-178.069	-4.44179	-3.15281	0.905662
52	O	22	21	19	1.383167	118.6006	-178.072	-0.50973	5.422607	0.905863
53	C	52	22	21	1.423905	114.275	-94.2307	0.442337	6.400145	0.499042
54	H	53	52	22	1.097594	111.4129	59.57856	0.40784	6.566134	-0.58538
55	H	53	52	22	1.092146	106.7126	178.7474	0.180159	7.327116	1.013601
56	H	53	52	22	1.097393	111.5007	-62.0873	1.462715	6.108477	0.778381
57	C	50	13	12	1.423913	114.2701	-93.9234	5.324739	-3.58067	0.496115
58	H	57	50	13	1.097583	111.4174	59.73437	5.491794	-3.62758	-0.58767
59	H	57	50	13	1.092146	106.7132	178.9027	6.256081	-3.81877	1.01447
60	H	57	50	13	1.0974	111.4939	-61.9328	4.561352	-4.32098	0.767181
61	C	51	6	5	1.423913	114.2758	-94.3076	-5.76431	-2.81781	0.497932
62	H	61	51	6	1.097596	111.4123	59.54092	-5.88996	-2.93066	-0.58659
63	H	61	51	6	1.092145	106.712	178.7094	-6.43595	-3.5088	1.011953
64	H	61	51	6	1.097389	111.5029	-62.1252	-6.02275	-1.78849	0.777166

Phosphine **4** (gas phase singlet electronic state; B3LYP-D3/6-31G(2d,p) with Grimme correction)

Tag	Symbol	NA	NB	NC	Bond	Angle	Dihedral	X	Y	Z
1	P							-0.09639	0.028676	1.582022
2	C	1			1.84284			0.713798	1.441002	0.71889
3	C	2	1		1.398132	117.559		1.795829	2.054507	1.357321
4	C	2	1	3	1.404525	124.6297	179.9384	0.321749	1.942104	-0.53326
5	C	3	2	1	1.394478	121.8293	178.9806	2.487205	3.116602	0.775495
6	C	5	3	2	1.397756	119.4241	0.790322	2.082949	3.597277	-0.4732
7	C	4	2	1	1.386555	121.0745	-179.464	0.992359	3.003832	-1.1211
8	C	1	2	3	1.843201	101.9341	-93.1148	0.801255	-1.41675	0.873246
9	C	8	1	2	1.405729	117.4748	167.4317	0.628437	-2.66073	1.504695
10	C	9	8	1	1.384941	121.3526	179.3739	1.254531	-3.80201	1.031871
11	C	10	9	8	1.400986	120.094	0.849327	2.094555	-3.73009	-0.08703
12	C	11	10	9	1.396985	119.5038	-0.15498	2.291715	-2.50118	-0.72146
13	C	12	11	10	1.396207	119.6948	-0.4137	1.643799	-1.36218	-0.23952
14	C	1	2	3	1.842943	101.915	162.1711	-1.7143	-0.07526	0.705674
15	C	14	1	2	1.398045	117.6701	-92.5251	-2.79276	0.63015	1.247759
16	C	14	1	2	1.404512	124.4968	87.38427	-1.93679	-0.81236	-0.46899
17	C	15	14	1	1.394385	121.8052	178.9193	-4.04937	0.62989	0.643404
18	C	17	15	14	1.397844	119.4344	0.790256	-4.24813	-0.10662	-0.52793
19	C	16	14	1	1.386506	121.0745	-179.391	-3.18269	-0.83085	-1.07709
20	H	15	14	1	1.086556	119.4577	-1.05418	-2.65419	1.196362	2.164714
21	H	16	14	1	1.084649	119.7189	0.687715	-1.12394	-1.37885	-0.9104
22	H	3	2	1	1.086555	119.4368	-1.00709	2.111613	1.698156	2.333991
23	H	4	2	1	1.084585	119.796	0.633313	-0.51949	1.496318	-1.0528
24	H	9	8	1	1.086506	119.5453	-0.54516	-0.00965	-2.73263	2.381147
25	H	13	12	11	1.084538	118.6875	-179.674	1.804347	-0.41764	-0.74774
26	O	11	10	9	1.360915	115.6104	179.5658	2.669307	-4.90353	-0.46752
27	O	6	5	3	1.360746	124.8281	179.5762	2.671098	4.629944	-1.13601
28	O	18	17	15	1.360617	124.8265	179.5909	-5.4268	-0.19057	-1.20244
29	C	28	18	17	1.416804	118.1155	0.223046	-6.5406	0.520547	-0.69146
30	H	29	28	18	1.097787	111.6483	60.96489	-6.35141	1.601466	-0.66047
31	H	29	28	18	1.091096	106.0799	179.8017	-7.36659	0.320624	-1.37575
32	H	29	28	18	1.09775	111.6452	-61.3709	-6.81415	0.176114	0.314316
33	C	26	11	10	1.41658	118.0873	-179.793	3.532483	-4.89008	-1.59066
34	H	33	26	11	1.097814	111.6496	61.13012	4.398745	-4.23564	-1.4279
35	H	33	26	11	1.091116	106.0879	179.9774	3.877995	-5.91708	-1.71879
36	H	33	26	11	1.097824	111.6563	-61.1871	3.008396	-4.5698	-2.50059
37	C	27	6	5	1.416767	118.1088	0.078095	3.776764	5.271714	-0.52538
38	H	37	27	6	1.097811	111.6536	61.07751	4.611367	4.576546	-0.36611
39	H	37	27	6	1.0911	106.0837	179.9152	4.090336	6.055987	-1.2161
40	H	37	27	6	1.097742	111.6444	-61.2509	3.501349	5.726088	0.435205
41	H	7	4	2	1.084499	121.3718	-179.848	0.692247	3.396146	-2.08658
42	H	5	3	2	1.082397	119.428	-179.792	3.321604	3.560631	1.302941
43	H	12	11	10	1.082568	121.0652	179.7182	2.938904	-2.41583	-1.58506
44	H	10	9	8	1.084296	121.5164	-179.736	1.119749	-4.76365	1.514333
45	H	19	16	14	1.084481	121.3847	-179.87	-3.36061	-1.39989	-1.98298
46	H	17	15	14	1.082397	119.4306	-179.777	-4.85657	1.192554	1.094424

PPh₃ (gas phase singlet electronic state; B3LYP-D3/6-31G(2d,p) with Grimme correction)

Tag	Symbol	NA	NB	NC	Bond	Angle	Dihedral	X	Y	Z
1	P							0	0	1.25656
2	C	1			2.77898			-2.69246	-0.64665	1.021509
3	H	2	1		1.086454	83.22531		-2.78201	-0.05185	1.92626
4	C	1	2	3	4.164961	128.3427	-178.533	3.137849	-1.04032	-1.27692
5	C	1	2	4	1.845884	99.83041	94.3692	0	1.652994	0.435038
6	C	4	1	5	1.393733	101.664	167.4361	3.592363	-2.22108	-0.69236
7	H	6	4	1	1.085313	120.1602	-179.971	4.42919	-2.75801	-1.12748
8	C	2	1	5	2.781518	97.01227	96.49513	-2.46987	-2.1973	-1.27692
9	C	2	1	5	1.392345	157.0888	94.81365	-3.8291	-1.22096	0.458629
10	C	5	1	2	1.40222	116.9883	139.4772	0.786217	2.65506	1.021509
11	H	10	5	1	1.086454	119.5141	-0.79197	1.346107	2.435217	1.92626
12	C	4	1	5	1.394116	18.62104	-12.6544	2.063073	-0.34857	-0.72024
13	H	12	4	1	1.084326	119.683	-179.68	1.713077	0.565425	-1.18701
14	C	8	2	1	1.393733	60.19541	-179.35	-3.7197	-2.00054	-0.69236
15	H	14	8	2	1.085313	120.1602	-179.532	-4.6031	-2.45679	-1.12748
16	C	8	2	1	1.394116	60.09127	0.178727	-1.33341	-1.61239	-0.72024
17	H	16	8	2	1.084327	119.6831	179.9498	-0.36687	-1.76628	-1.18701
18	C	16	8	2	1.400683	120.507	-0.15681	-1.43154	-0.8265	0.435038
19	C	12	4	1	1.400683	120.507	0.213865	1.431535	-0.8265	0.435038
20	C	6	4	1	1.394446	119.7013	-0.33437	2.971929	-2.70562	0.458629
21	C	10	5	1	2.41362	90.78954	179.6462	0.127332	4.221618	-0.69236
22	H	21	10	5	1.085314	150.1023	179.7341	0.173914	5.214798	-1.12748
23	C	21	10	5	1.393733	89.7342	0.545889	-0.66798	3.237619	-1.27692
24	C	10	5	1	1.392345	120.804	179.2219	0.857172	3.926577	0.458629
25	C	20	6	4	1.392344	120.0156	-0.21021	1.906241	-2.00841	1.021509
26	H	25	20	6	1.086454	119.6819	-179.138	1.435906	-2.38337	1.92626
27	C	23	21	10	1.394115	120.285	-0.4729	-0.72966	1.960961	-0.72024
28	H	27	23	21	1.084326	119.683	-179.577	-1.34621	1.200856	-1.18701
29	H	20	6	4	1.085425	120.1623	-179.668	3.323243	-3.62156	0.923145
30	H	4	1	5	1.085611	138.2627	-12.8064	3.617973	-0.65636	-2.17169
31	H	8	2	1	1.08561	179.6535	39.80054	-2.37741	-2.80508	-2.17169
32	H	9	2	1	1.085425	119.8199	-178.509	-4.79799	-1.06723	0.923145
33	H	23	21	10	1.08561	120.073	179.7473	-1.24056	3.461437	-2.17169
34	H	24	10	5	1.085425	119.8199	-179.692	1.474745	4.688795	0.923145

References for the Supporting Information

1. F. H. Allen, *Acta Crystallogr., Sect. B: Struct. Sci.* **2002**, *58*, 380–388.
2. B. Laleu, G. Bernardinelli, R. Chauvin, J. Lacour, *J. Org. Chem.* **2006**, *71*, 7412–7416.
3. Gaussian 03, Revision C.02, M. J. Frisch, G. W. Trucks, H. B. Schlegel, G. E. Scuseria, M. A. Robb, J. R. Cheeseman, J. A. Montgomery, Jr., T. Vreven, K. N. Kudin, J. C. Burant, J. M. Millam, S. S. Iyengar, J. Tomasi, V. Barone, B. Mennucci, M. Cossi, G. Scalmani, N. Rega, G. A. Petersson, H. Nakatsuji, M. Hada, M. Ehara, K. Toyota, R. Fukuda, J. Hasegawa, M. Ishida, T. Nakajima, Y. Honda, O. Kitao, H. Nakai, M. Klene, X. Li, J. E. Knox, H. P. Hratchian, J. B. Cross, V. Bakken, C. Adamo, J. Jaramillo, R. Gomperts, R. E. Stratmann, O. Yazyev, A. J. Austin, R. Cammi, C. Pomelli, J. W. Ochterski, P. Y. Ayala, K. Morokuma, G. A. Voth, P. Salvador, J. J. Dannenberg, V. G. Zakrzewski, S. Dapprich, A. D. Daniels, M. C. Strain, O. Farkas, D. K. Malick, A. D. Rabuck, K. Raghavachari, J. B. Foresman, J. V. Ortiz, Q. Cui, A. G. Baboul, S. Clifford, J. Cioslowski, B. B. Stefanov, G. Liu, A. Liashenko, P. Piskorz, I. Komaromi, R. L. Martin, D. J. Fox, T. Keith, M. A. Al-Laham, C. Y. Peng, A. Nanayakkara, M. Challacombe, P. M. W. Gill, B. Johnson, W. Chen, M. W. Wong, C. Gonzalez, and J. A. Pople, Gaussian, Inc., Wallingford CT, 2004.
4. Gaussian 16, Revision B.01, M. J. Frisch, G. W. Trucks, H. B. Schlegel, G. E. Scuseria, M. A. Robb, J. R. Cheeseman, G. Scalmani, V. Barone, G. A. Petersson, H. Nakatsuji, X. Li, M. Caricato, A. V. Marenich, J. Bloino, B. G. Janesko, R. Gomperts, B. Mennucci, H. P. Hratchian, J. V. Ortiz, A. F. Izmaylov, J. L. Sonnenberg, D. Williams-Young, F. Ding, F. Lipparini, F. Egidi, J. Goings, B. Peng, A. Petrone, T. Henderson, D. Ranasinghe, V. G. Zakrzewski, J. Gao, N. Rega, G. Zheng, W. Liang, M. Hada, M. Ehara, K. Toyota, R. Fukuda, J. Hasegawa, M. Ishida, T. Nakajima, Y. Honda, O. Kitao, H. Nakai, T. Vreven, K. Throssell, J. A. Montgomery, Jr., J. E. Peralta, F. Ogliaro, M. J. Bearpark, J. J. Heyd, E. N. Brothers, K. N. Kudin, V. N. Staroverov, T. A. Keith, R. Kobayashi, J. Normand, K. Raghavachari, A. P. Rendell, J. C. Burant, S. S. Iyengar, J. Tomasi, M. Cossi, J. M. Millam, M. Klene, C. Adamo, R. Cammi, J. W. Ochterski, R. L. Martin, K. Morokuma, O. Farkas, J. B. Foresman, and D. J. Fox, Gaussian, Inc., Wallingford CT, 2016.
5. GaussView, Version 6, Roy Dennington, Todd A. Keith, and John M. Millam, Semichem Inc., Shawnee Mission, KS, 2016.